Lattice dynamics study of scheelite tungstates under high pressure II. $PbWO_4$

F. J. Manjon,[1,2,*] D. Errandonea,[1] N. Garro,[1] J. Pellicer-Porres,[1] J. López-Solano,[3] P. Rodríguez-Hernández,[3] S. Radescu,[3] A. Mujica,[3] and A. Muñoz[3]

[1]*Departamento de Física Aplicada i Institut de Ciencia de Materials de la Universitat de València, 46100 Burjassot (València), Spain*

[2]*Departamento de Física Aplicada, Universitat Politècnica de València, 46022 València, Spain*

[3]*Departamento de Física Fundamental II, Universidad de La Laguna, La Laguna 38205, Tenerife, Spain*

(Received 21 June 2006; revised manuscript received 19 July 2006; published 31 October 2006)

Room-temperature Raman scattering has been measured in lead tungstate up to 17 GPa. We report the pressure dependence of all the Raman modes of the tetragonal scheelite phase ($PbWO_4$-I or stolzite, space group $I4_1/a$), which is stable at ambient conditions. Upon compression the Raman spectrum undergoes significant changes around 6.2 GPa due to the onset of a partial structural phase transition to the monoclinic $PbWO_4$-III phase (space group $P2_1/n$). Further changes in the spectrum occur at 7.9 GPa, related to a scheelite-to-fergusonite transition. This transition is observed due to the sluggishness and kinetic hindrance of the I→III transition. Consequently, we found the coexistence of the scheelite, $PbWO_4$-III, and fergusonite phases from 7.9 to 9 GPa, and of the last two phases up to 14.6 GPa. We have performed *ab initio* lattice-dynamics calculations, which have greatly helped us in assigning the Raman modes of the three phases and discussing their pressure dependence. The Raman modes of the free WO_4 molecule are discussed.

DOI: 10.1103/PhysRevB.74.144112 PACS number(s): 62.50.+p, 63.20.−e, 78.30.−j

I. INTRODUCTION

Lead tungstate ($PbWO_4$) has been proposed as an excellent material for the implementation of Raman lasers due to the strong-scattering cross section of the highest A_{1g} mode of the scheelite structure.[1] It is also one of the candidate materials chosen for the cryogenic phonon-scintillation detectors at the high-energy electromagnetic calorimeter of the Large Hadron Collider at CERN.[2,3] For both applications a detailed knowledge of its lattice dynamics and structural properties is highly desirable.

$PbWO_4$ is a compound that crystallizes in the tetragonal scheelite-type structure [$PbWO_4$-I or stolzite, space group (SG): $I4_1/a$, No. 88, $Z=4$] at ambient conditions.[4] However, other two-metastable polymorphs have also been observed: raspite-type ($PbWO_4$-II, SG: $P2_1/a$, No. 14, $Z=4$),[5,6] and $PbWO_4$-III (SG: $P2_1/n$, No. 14, $Z=8$).[7] The raspite phase coexists with the scheelite phase in some natural samples. On the other hand, the $PbWO_4$-III phase can only be obtained after a high-pressure high-temperature treatment and several authors have proposed this phase as a candidate high-pressure phase at room temperature (RT) in $PbWO_4$.[8,9]

As already commented in part I of this study,[10] the behavior of scheelite-type tungstates under pressure has been studied since the 1970s. Recently a systematic study of their structure under high pressure has been performed in alkaline-earth tungstates and $PbWO_4$ by means of angle-dispersive x-ray diffraction (ADXRD) and x-ray absorption near-edge structure (XANES) measurements in powder samples, complemented with *ab initio* total-energy calculations.[11,12] It has been found that scheelite $PbWO_4$ transforms under pressure to the monoclinic *M*-fergusonite structure (hereafter called fergusonite, SG: $I2/a$, No. 15, $Z=4$) at 9.0 GPa.[12] This transition pressure is in good agreement with the value estimated for $PbWO_4$ from the correlation of the transition pressures with the packing ratio of anionic BX_4 units around *A* cations in scheelite-related ABX_4 compounds.[13] In Ref. 12 it was also found that $PbWO_4$ undergoes a second phase transition to the monoclinic $PbWO_4$-III phase around 15 GPa. The presence of two phase transitions in $PbWO_4$ has been confirmed by recent optical measurements under pressure.[14] However, there is still some controversy concerning the high-pressure phases of $PbWO_4$. *Ab initio* total-energy calculations indicated that $PbWO_4$-III is the energetically most favored structure beyond 5.3 GPa and should be the only phase observed at least up to 20 GPa because the fergusonite structure is more stable than a scheelite one only beyond 8 GPa.[12] The controversy is even more evident if we consider that an early Raman study[9] and a recent ADXRD study[15] in $PbWO_4$ showed indications of a phase transition at 4.5 and 5 GPa, respectively, but there are some puzzling questions regarding these works. In Ref. 15, the ADXRD patterns have been assigned to stolzite up to 10 GPa, despite the observation of subtle changes at 5 GPa. Furthermore, in that work the observed new weak reflections cannot be accounted for either by the fergusonite or the $PbWO_4$-III structures. On the other hand, in the Raman study,[9] it was suggested that the high-pressure phase of $PbWO_4$ could be different than that of $BaWO_4$ because of the different Raman-mode frequencies observed in the high-pressure phase of both materials. However, no Raman spectrum of the high-pressure phase of $PbWO_4$ was provided in Ref. 9 to compare it with that of $BaWO_4$. On top of that, some Raman modes of the scheelite phase were not found in that work. Therefore, the lack of high-pressure Raman spectra in $PbWO_4$, the absence of some first-order modes of the scheelite structure, and the apparent discrepancies among earlier experimental and theoretical works justify our present study.

As part of our project to study the stability of scheelite-structured tungstates and to give a comprehensive description of their complex high-pressure phase diagrams, we report in this paper a study of the lattice dynamics of $PbWO_4$ up to 17 GPa. We provide Raman measurements and *ab initio* lattice dynamics calculations for $PbWO_4$ in order to as-

sign and discuss the behavior of the zone-center phonons in the different structural phases. This paper complements part I devoted to $BaWO_4$,[10] in which it was shown that the onset of a partial scheelite-to-$BaWO_4$-II phase transition occurs at lower pressure (6.9 GPa) than the scheelite-to-fergusonite transition (7.5 GPa) in good agreement with previous *ab initio* total-energy calculations and ADXRD and XANES measurements.[12] In this paper we will show that $PbWO_4$ suffers the same phase transitions as $BaWO_4$ and that the frequencies of the Raman modes in the high-pressure phases of $PbWO_4$ previously reported[9] can be completely understood in the light of the present study. Our results allow us to develop a picture of the structural behavior of $PbWO_4$ that solves apparent discrepancies among earlier experiments and theory.

II. EXPERIMENTAL DETAILS

The $PbWO_4$ samples used in this study were scheelite-type bulk single crystals grown with the Czochralski method starting from raw powders having 5*N* purity.[16,17] The preparation of samples is similar to that of Ref. 10. Silicone oil was used as a pressure-transmitting medium inside the diamond anvil cell (DAC).[18] Raman measurements at RT under pressure were performed in backscattering geometry in the same way as described in Ref. 10.

III. *Ab initio* LATTICE DYNAMICS CALCULATIONS

Along with the experimental Raman spectra we will also present results of a theoretical *ab initio* calculation of the phonon modes of the scheelite, fergusonite, and $PbWO_4$-III phases at the zone center (Γ point). All the calculations were done within the framework of the density functional theory (DFT) using the Vienna *ab initio* simulation package (VASP),[19] as described in Ref. 10. The projector-augmented wave (PAW) scheme[20] was adopted and the semicore 5*d* electrons of Pb were dealt with explicitly in the calculations. The set of plane waves used extended up to a kinetic-energy cutoff of 625 eV. We perform highly converged calculations in order to obtain the dynamical matrix as described in Ref. 10.

IV. RESULTS AND DISCUSSION

A. Low-pressure phase: Scheelite structure

$PbWO_4$ crystallizes at ambient conditions in the centrosymmetric scheelite structure that has the space group $I4_1/a$ (C_{4h}^6), with four formula units per body-centered unit cell. The Pb and W atoms occupy S_4 sites whereas the sixteen oxygen atoms are on general C_1 sites. Group theoretical considerations[21–23] lead us to expect 13 Raman active modes at the Γ point;[10]

$$\Gamma = \nu_1(A_g) + \nu_2(A_g) + \nu_2(B_g) + \nu_3(B_g) + \nu_3(E_g) + \nu_4(B_g) + \nu_4(E_g) + R(A_g) + R(E_g) + 2T(B_g) + 2T(E_g). \quad (1)$$

The translational modes (T) and the rotational modes (R) are considered to be the external modes of the WO_4 tetrahedra and are the lowest in frequency. The rest (ν_1 to ν_4) are considered to be the internal modes of the WO_4 tetrahedra and higher in frequency. The A_g and B_g modes are single, while E_g modes are doubly degenerated.

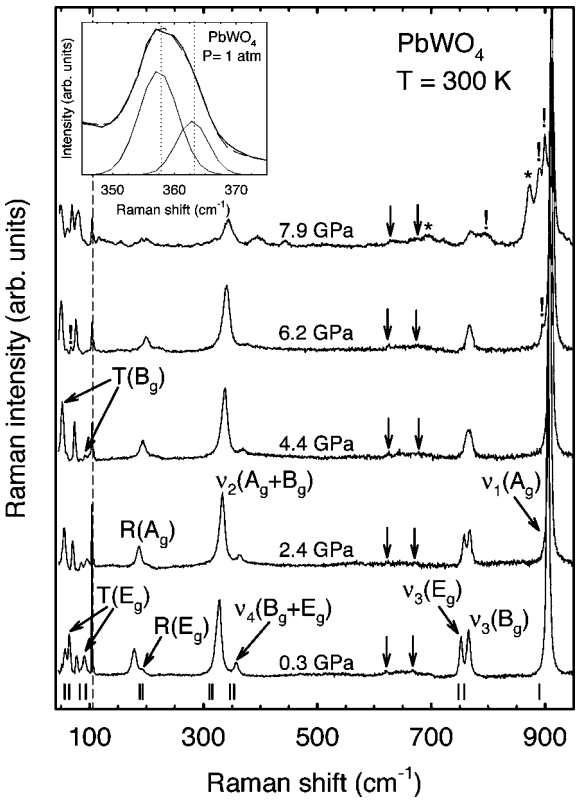

FIG. 1. RT Raman spectra of scheelite $PbWO_4$ at different pressures between 1 atm and 8 GPa. The dashed line indicates the position of a plasma line of Ar^+ at 104 cm^{-1} used for the calibration of Raman spectra. Arrows indicate the position of the silicon oil modes at different pressures. The inset shows a detail of the Raman spectrum at 1 atm in the region of the $\nu_4(B_g)$ and $\nu_4(E_g)$ modes. The exclamation marks indicate the Raman peaks assigned to the $PbWO_4$-III phase. Asterisks indicate the Raman peaks assigned to the fergusonite phase. The *ab initio* calculated frequencies of the scheelite Raman modes at 1 atm are marked at the bottom.

To the best of our knowledge twelve of the thirteen modes of the scheelite-type phase of $PbWO_4$ are known,[24,25] the $\nu_4(E_g)$ internal mode being the only unknown one. This mode has been observed in $CaWO_4$, $SrWO_4$, and $BaWO_4$ as a high-frequency shoulder of the $\nu_4(B_g)$ internal mode.[10,26,27] Only the pressure dependence of ten of the thirteen modes is known.[9] Figure 1 shows the *RT* Raman spectra of stolzite at different pressures up to 8 GPa. The Raman spectra should correspond to a mixture of polarizations perpendicular and parallel to the *c* axis because of our sample orientation. In order to assign the different Raman modes of stolzite we have followed the notation of Liegeois-Duyckaerts and Tarte.[28] Marks at the bottom of Fig. 1 indicate the *ab initio*-calculated frequencies of the Raman modes in scheelite $PbWO_4$ at 1 atm. It can be seen that our experimental and theoretical Raman frequencies at 1 atm compare reasonably well. The Raman spectrum of stolzite is dominated by the $\nu_1(A_g)$ mode near 906 cm^{-1} at 1 atm; i.e., the mode used in

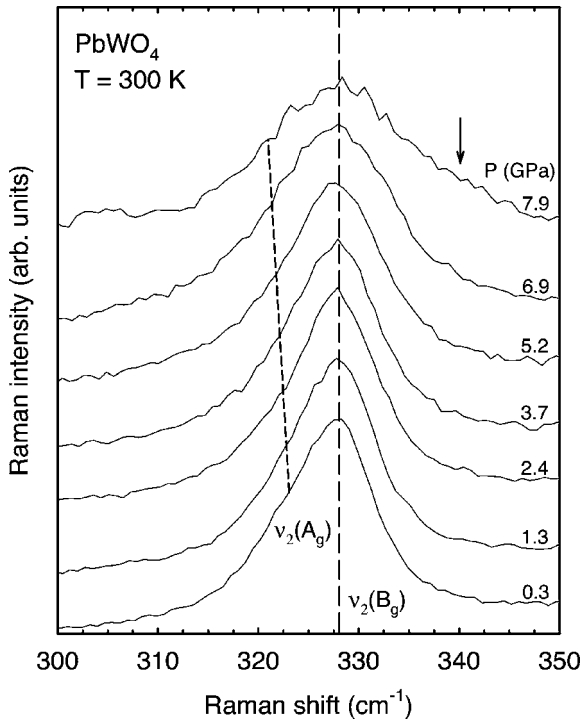

FIG. 2. Detail of the Raman spectra of scheelite $PbWO_4$ at different pressures around the $\nu_2(B_g)$ mode. Raman spectra above 0.3 GPa have been shifted by −1.97, −5.53, −8.45, −11.21, −13.80, and −15.42 cm^{-1}, respectively, in order to bring the mode at 328 cm^{-1} (long-dashed line) into coincidence. The short-dashed line indicates the relative evolution of the low-frequency mode at 323 cm^{-1} at 1 atm with respect to the 328 cm^{-1} line. The arrow indicates a mode of the fergusonite phase, which begins to appear in the spectrum around 8 GPa.

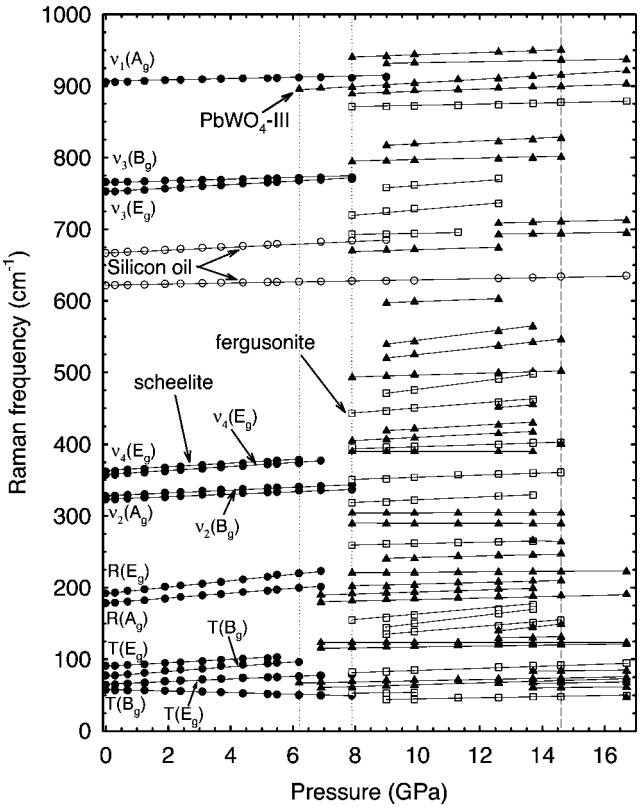

FIG. 3. Pressure dependence of the Raman mode frequencies of the stolzite (solid circles), fergusonite (empty squares), and $PbWO_4$-III (solid triangles) phases of $PbWO_4$ up to 17 GPa. Empty circles show the pressure behavior of the two silicon-oil Raman modes observed. The dotted lines show the onset of the scheelite-to-$PbWO_4$-III phase transition and of the scheelite-to-fergusonite transition. The dashed line indicates the pressure for the completion of the transition to the $PbWO_4$-III phase. The solid lines are guides to the eye.

Raman lasers. In addition, one can distinguish clearly at least ten other modes in the experimental Raman spectrum of the scheelite phase. Only two modes (one ν_2 and one ν_4 mode) cannot be clearly observed because they probably overlap with other modes, as can be inferred from the proximity of the calculated ν_2 and ν_4 frequencies (see the bottom of Fig. 1). A closer inspection of the modes located near 328 and 357 cm^{-1} at 1 atm allows us to conclude that they are indeed double modes. The inset of Fig. 1 shows a detailed Raman spectrum of the region near 357 cm^{-1} at 1 atm measured outside the DAC. We have found a mode at 363 cm^{-1} at 1 atm as a high-frequency shoulder of the $\nu_4(B_g)$ mode near 357 cm^{-1}. In a similar fashion, we have found a mode at 323 cm^{-1} at 1 atm as a low-frequency shoulder of the $\nu_2(B_g)$ mode located at 328 cm^{-1} at 1 atm. Figure 2 shows a detail of the Raman spectra near the $\nu_2(B_g)$ mode at several pressures. The spectra at different pressures have been shifted in frequency in order to bring the $\nu_2(B_g)$ mode into coincidence, so that the relative shift of the low-frequency shoulder with respect to the $\nu_2(B_g)$ mode as a function of pressure can be observed. The low-frequency tail of the anisotropic $\nu_2(B_g)$ mode linewidth becomes more pronounced with increasing pressure. This feature can be attributed to the presence of the $\nu_2(A_g)$ mode at the low-frequency side of the $\nu_2(B_g)$ mode. In summary, we have tentatively assigned the modes located at 323 and 367 cm^{-1} to the $\nu_2(A_g)$ mode and the unreported $\nu_4(E_g)$ mode in scheelite-type $PbWO_4$, respectively. The assignment of the $\nu_2(A_g)$ mode is based on the ordering of the two modes and on the slightly smaller pressure coefficient of the $\nu_2(A_g)$ mode with respect to the $\nu_2(B_g)$ mode, as indicated by our lattice-dynamics calculations, and previously commented on in the case of scheelite-$BaWO_4$.[10] The assignment of the $\nu_4(E_g)$ mode is based on its location, on its similar pressure coefficient to that of the $\nu_4(B_g)$ mode, according to our calculations, and on the similar location of this mode in $CaWO_4$, $SrWO_4$, and $BaWO_4$.[10,26,27] Further support for the assignment of the previously unobserved ν_2 and ν_4 modes comes from the knowledge that the intensity of the ν_2 modes must be higher than those of ν_4 modes,[29] and that the lack of observation of several Raman ν_2 and/or ν_4 modes in tetrahedral ABO_4-type compounds is due to the fact that the ν_2 and/or ν_4 frequencies almost coincide,[30] as indeed found in our calculations.

Figure 3 shows the pressure dependence of the Raman-mode frequencies of stolzite (solid circles) up to 8 GPa. Table I summarizes the frequencies (ω) of all the stolzite Raman modes, their pressure coefficients ($d\omega/dP$), and Grü-

TABLE I. *Ab initio* calculated and experimental frequencies, pressure coefficients, and Grüneisen parameters of the Raman modes of scheelite $PbWO_4$ at 1 atm. For obtaining the Grüneisen parameter, $\gamma = B_0/\omega(0)\cdot d\omega/dP$, we have taken the bulk modulus of scheelite $PbWO_4$, B_0=66 GPa (Ref. 12).

Peak/mode	$\omega(0)$ cm^{-1}	$d\omega/dP$ cm^{-1}/GPa	γ	$\omega(0)^c$ cm^{-1}	$d\omega/dP^c$ cm^{-1}/GPa	γ^c
$T(B_g)$	58	−1.1	−1.3,[a] −1.10[b]	52	0.7	0.81
$T(E_g)$	65	1.8	1.8,[a] 3.20[b]	64	2.3	2.37
$T(B_g)$	77	3.3	2.8,[a] 2.20[b]	79	4.4	3.67
$T(E_g)$	90	2.3	1.7,[a] 1.70[b]	92	4.6	3.30
$R(A_g)$	178	3.3	1.2,[a] 1.40[b]	191	3.3	1.14
$R(E_g)$	193	4.2	1.4[a]	193	4.6	1.57
$\nu_2(A_g)$	323	1.9	0.4[a]	310	2.1	0.45
$\nu_2(B_g)$	328	2.1	0.4,[a] 0.60[b]	311	3.0	0.64
$\nu_4(B_g)$	357	2.8	0.5,[a] 0.60[b]	350	2.7	0.51
$\nu_4(E_g)$	362	2.7	0.5[a]	351	2.8	0.53
$\nu_3(E_g)$	752	2.4	0.2,[a] 0.30[b]	750	3.1	0.27
$\nu_3(B_g)$	766	0.9	0.08,[a] 0.05[b]	758	1.7	0.15
$\nu_1(A_g)$	906	0.8	0.06,[a] 0.08[b]	890	1.4	0.10

[a]This work.
[b]Reference 9.
[c]*Ab initio* calculations.

neisen parameters ($\gamma = B_0/\omega\cdot d\omega/dP$, with B_0=66 GPa being the stolzite bulk modulus[12]). In Table I, we also compare the experimental results for stolzite with those obtained from our calculations. For completeness, Table II summarizes the calculated frequencies and pressure coefficients of the infrared (IR) modes of stolzite that compare reasonably well to the experimental frequencies obtained from the literature.[26,27,33]

TABLE II. Frequencies, pressure coefficients, and Grüneisen parameters of the calculated IR modes in scheelite $PbWO_4$ at 1 atm. Experimentally measured IR active modes at *RT* are also reported for comparison. The values for the silent B_u modes are also shown for completeness.

Peak/mode	$\omega(0)$ (cm^{-1})	$d\omega/dP$ (cm^{-1}/GPa)	γ	$\omega(0)$ experimental (cm^{-1})
$T(A_u)$	0			0
$T(E_u)$	0			0
$T(E_u)$	54	7.0	8.5	58[a]
$T(A_u)$	71	7.1	6.6	73[a]
$R(E_u)$	122	−0.8	−0.4	104[a]
$R(B_u)$	222	0.3	0.09	
$\nu_4(A_u)$	243	−2.1	−0.6	251[a]
$\nu_4(E_u)$	275	1.8	0.4	288[a]
$\nu_2(A_u)$	370	2.5	0.5	384[a]
$\nu_2(B_u)$	385	5.2	0.9	
$\nu_3(A_u)$	746	2.4	0.2	756,[a] 757[c]
$\nu_3(E_u)$	754	2.6	0.2	764,[a] 771[c]
$\nu_1(B_u)$	891	2.0	0.15	862,[b] 850[c]

[a]Reference 24.
[b]Reference 31.
[c]Reference 25.

Our measured Raman frequencies, pressure coefficients, and Grüneisen parameters in scheelite $PbWO_4$ agree with those reported by Jayaraman *et al.*[9] The only significant deviation corresponds to pressure coefficients measured for the lowest $T(E_g)$ mode at 65 cm^{-1} and the $T(B_g)$ mode at 77 cm^{-1}. We have measured a much smaller pressure coefficient (1.8 cm^{-1}/GPa) for the $T(E_g)$ mode than that measured previously (3.4 cm^{-1}/GPa).[9] Consequently, our pressure coefficient gives a Grüneisen parameter γ of 1.9 that is much smaller than the 3.2 obtained by Jayaraman *et al.*[9] Note that there is a mistake in Table I of Ref. 9 and the reported Grüneisen parameters of $PbWO_4$ and $PbMoO_4$ are underestimated by an order of magnitude. Our pressure coefficient for the lowest $T(E_g)$ mode is similar to those in other scheelite tungstates (between 1 and 1.7 cm^{-1}/GPa) and our γ is in agreement with those found for this mode in other scheelite tungstates (between 1 and 1.4).[10] As regards our γ for the $T(B_g)$ mode at 77 cm^{-1} (2.8), it seems to be rather high as compared to the same mode in other scheelites,[8–10] but the pressure coefficient (3.26 cm^{-1}/GPa) is remarkably similar to that recently measured for the highest $T(B_g)$ phonon (3.4 cm^{-1}/GPa) in $SrWO_4$,[26] and even smaller than the same mode in $CaWO_4$ (4.7 cm^{-1}/GPa).[27] It must be noted that this mode was not observed in the oldest Raman studies on scheelite tungstates under pressure.[32,33] The small γ for this mode in stolzite is due to the strong decrease of its frequency at 1 atm in the tungstate series (Ca, Sr, Ba, Pb).[28] In fact, the Grüneisen parameters for the three lowest frequency modes in stolzite are much larger than those of the same modes in alkaline-earth scheelites because of the smaller frequencies of those modes in $PbWO_4$. In fact, the frequencies of all the external *T* modes in scheelite tungstates are inversely proportional to the square root of the cation mass due to the negli-

gible contribution of the WO_4 tetrahedron to the frequency of these modes, and consequently decrease smoothly in the Sr, Ba, Pb series. However, this not the case for the highest $T(B_g)$ phonon, which suffers an exceptional decrease in frequency from 133 cm^{-1} in $BaWO_4$ to 77 cm^{-1} in $PbWO_4$.[28]

One common assumption in ABO_4-type scheelites regarding the pressure coefficients of their Raman modes is that the relatively stable tetrahedral BO_4 units are not as affected by pressure as dodecahedral AO_8 units, and consequently the pressure coefficients of the WO_4 tetrahedra internal modes should be smaller than those of the external modes. In this sense, we must note that $PbWO_4$ follows this trend more closely than alkaline-earth tungstates (see Table I in this work and in Ref. 10). It can also be observed that the pressure coefficients of all internal modes in $PbWO_4$ are smaller than those in the alkaline-earth tungstates. We believe that this result could be due to the smaller ionicity of the $PbWO_4$ with respect to the alkaline-earth tungstates, as discussed below.

It is known that the frequency of the stretching modes in WO_4 depends on the square root of the bonding force constant k, which increases with the intensity of the W-O interaction and decreases with the W-O bond distance. In general, a pressure increase should not alter the intensity of the W-O interaction very much, but reduces the bond distance resulting in an increase of the force constant, and consequently of the frequency. However, the W-O bond compressibility usually decreases with an increase in the compound ionicity because the W-O bond compressibility decreases with an increase in the charge transfer from the A^{2+} cation to the WO_4^{2-} anion. The consideration of the above statements and the observation of rather different pressure coefficients for the stretching $\nu_1(A_g)$ mode in the four scheelite AWO_4 tungstates (A=Ca, Sr, Ba, Pb) suggest a different behavior of the W-O interaction or of the W-O bond distance under pressure in the four tungstates, in particular, between the most ionic ($BaWO_4$) and the least ionic compound ($PbWO_4$). Since $BaWO_4$ and $PbWO_4$ have similar W-O bond compressibilities,[12,13] the only explanation for the factor 3 between the relative pressure coefficients of the stretching $\nu_1(A_g)$ mode in these two compounds is that it must be a change in the intensity of the W-O interaction in these tungstates with increasing pressure.

In order to complete the understanding of the pressure dependence of the Raman modes in stolzite in comparison with scheelite alkaline-earth tungstates, let us analyze further the high-frequency stretching modes of this phase. All the asymmetric stretching ν_3 modes have similar frequencies and pressure coefficients in $CaWO_4$, $SrWO_4$, and $BaWO_4$.[10] In these compounds, the frequency (pressure coefficient) is near 797 cm^{-1} (3 cm^{-1}/GPa) and near 835 cm^{-1} (2 cm^{-1}/GPa) for the $\nu_3(E_g)$ and the $\nu_3(B_g)$ modes, respectively. In $PbWO_4$, these frequencies are 5 to 8% smaller and their pressure coefficients are 25 to 50% smaller. On the other hand, the frequency and pressure coefficient of the symmetric stretching $\nu_1(A_g)$ mode increases from 911 to 926 cm^{-1} and from 1.5 to 2.7 cm^{-1}/GPa, respectively, when going from $CaWO_4$ to $BaWO_4$.[10] This evolution suggests a dependence of the $\nu_1(A_g)$ mode on A cation parameters, despite the fact that this mode is an internal mode of the WO_4 tetrahedra and should be basically independent of the A cation, as already mentioned. The dependence of the frequency of the $\nu_1(A_g)$ mode on the A cation was confirmed by Dean *et al.* from Raman and IR measurements in aqueous solutions.[34] The comparison of the frequencies and pressure coefficients of the $\nu_1(A_g)$ mode in alkaline-earth tungstates with those in $PbWO_4$ suggests that the scaling of this mode does not depend on the A cation mass or ionic radius, but on the ionicity of the compound. The ionicity of the AWO_4 compound depends on the electronegativity of the A^{2+} cation with respect to the WO_4^{2-} anion. Ordering the A^{2+} cations in increasing electronegativity (Ba^{2+}, Sr^{2+}, Ca^{2+}, Pb^{2+}) correlates with the decrease of the frequency and pressure coefficient of the stretching $\nu_1(A_g)$ mode, thus indicating that the smaller ionicity of $PbWO_4$, as compared to the alkaline-earth tungstates, leads to smaller frequencies and pressure coefficients of the internal stretching vibrations of the WO_4 molecule in $PbWO_4$ than in alkaline-earth tungstates.

Additional support for the dependence of the stretching frequencies on the compound ionicity is obtained from the frequencies measured in several BO_4 molecules: (1) the ν_1 and ν_3 frequencies increase with the cation valence in the $[WO_4]^{4-}$ to $[WO_4]^{2-}$ series; (2) the ν_1 and ν_3 frequencies increase with the cation mass in the $[CrO_4]^{2-}$, $[MoO_4]^{2}$, $[WO_4]^{2-}$ series; and (3) the ν_1 and ν_3 frequencies increase with the cation valence in the $[WO_4]^{2-}$, $[ReO_4]^{-}$, $[OsO_4]$ series, with W, Re, and Os belonging to the same row in the Periodic Table.[35] All these results cannot be connected to mass effect since heavier masses of cations would tend to smaller frequencies, which is not the case. The above results indicate that the stretching force constants in BO_4 tetrahedral molecules depend on the oxidation state of the B cation and consequently on the charge density of the BO_4 molecule, which is affected by the compound ionicity. The increase of the stretching force constant with increasing the oxidation state of the B cation (or with a higher charge density in the BO_4 tetrahedra) is due to the higher degree of $\sigma+\pi$ bonding between the B cation and the O anion present for the higher oxidation states (or for higher charge densities).[36] In particular, in scheelite tungstates the Raman and IR ν_1 and ν_3 frequencies are different for each compound and the compound with the largest ionicity ($BaWO_4$); i.e., with the largest charge transfer from the A^{2+} cation to the WO_4^{2-} anion, gives the largest ν_1 and ν_3 frequencies. Note that the ν_3 frequencies are almost equal in all three alkaline-earth tungstates. On the other hand, the smaller ν_1 and ν_3 frequencies in $PbWO_4$, as compared to $CaWO_4$, $SrWO_4$, and $BaWO_4$, are likely due to the more softened W-O bond in $PbWO_4$ since the W-O distances are pretty similar in the four tungstates.[11,12] In summary, we think that the stretching force constant in scheelite tungstates depends on the charge density of the WO_4 molecule, which is affected by the electronegativity of the A cation.

The WO_4 molecule has not yet been isolated in nature, therefore the internal modes A_1, E, and $2F_2$ of the WO_4 molecule, usually named as ν_1, ν_2, ν_3, and ν_4,[10,23] are not known. Raman measurements of tungstates solved in water give the following frequencies for the quasifree WO_4 molecule:[29,34,35]

$$\nu_1 = 931\ \text{cm}^{-1}, \quad \nu_2 = 325\ \text{cm}^{-1},$$

$$\nu_3 = 838\ \text{cm}^{-1}, \quad \nu_4 = 325\ \text{cm}^{-1}. \tag{2}$$

However, the proven dependence of the stretching frequencies of the WO_4 molecule on the ionicity of the material and the fact that H_2O is a polar solvent that can transfer charge to the WO_4^{2-} molecules cast a reasonable doubt about the validity of the above values as those corresponding to the quasifree WO_4 molecule. In this sense, we must note that the stretching ν_1 frequency for the quasifree WO_4 molecule measured in water (931 cm^{-1}) is even higher than that measured in $BaWO_4$ (926 cm^{-1}). Therefore, we conclude that the most approximate frequencies for the free WO_4 molecule, neglecting the distortion of the WO_4 tetrahedra in the solid compounds, are those found in $PbWO_4$, which is the tungstate compound with smaller ionicity. In summary, we propose that the Raman modes of the isolated WO_4 tetrahedra must be rather similar to the following ones:

$$\nu_1 = 906\ \text{cm}^{-1}, \quad \nu_2 = 325\ \text{cm}^{-1},$$

$$\nu_3 = 760\ \text{cm}^{-1}, \quad \nu_4 = 360\ \text{cm}^{-1}. \tag{3}$$

The same reasoning can be applied to other scheelite compounds, such as scheelite molybdates, and conclude that the most approximate frequencies for the free MoO_4 molecule are those found in scheelite $PbMoO_4$. The small Davydov splittings (or factor-group splittings) of the internal modes of the WO_4 molecule in stolzite give support for the assignment of the average frequencies of stolzite to the quasifree WO_4 molecule. Even though in the free WO_4 molecule there should be no Davydov splitting of the ν_2, ν_3, and ν_4 modes due to the interaction of equivalent interacting WO_4 molecules inside a unit cell, stolzite exhibits the smallest splittings of the known scheelite tungstates. In stolzite the Raman ν_2 splitting is 5 cm^{-1}, the ν_3 splitting is 14 cm^{-1}, and the ν_4 splitting is 5 cm^{-1} (see Table I). As regards the IR splittings, the ν_3 splitting is about 8 cm^{-1}, and the ν_4 splitting is 28 cm^{-1} (see Table II). These splittings are considerably smaller than those in the scheelite alkaline-earth tungstates.[10] In particular, the ν_3 splitting in the scheelite structure comes from the nonequivalence of the interactions of the four W-O bonds in the distorted tetrahedron. Therefore, the small ν_3 splitting in $PbWO_4$ is indeed indicative of the small distortion of the WO_4 tetrahedron, as compared to that in scheelite alkaline-earth tungstates, as should be expected in a quasifree WO_4 molecule.

Finally, to close this section we want to point out that we have observed several faint modes in the Raman spectrum at low pressures that are located at 621.4 cm^{-1} and at 666.5 cm^{-1} at 1 atm (see the arrows in Figs. 1 and 4). These modes have frequency pressure coefficients of 1.0 and 2.3 $\text{cm}^{-1}\ \text{GPa}^{-1}$, respectively, and their behaviors under pressure are displayed with open circles in Fig. 3. We have attributed these two Raman modes to the symmetric and asymmetric stretching modes of the silicon oil-pressure medium since $Si(\text{-O-}CH_3)_n$ and $Si\text{-}CH_3$ chains of dimethylsiloxanes and trimethylsiloxanes in silicon oils are in the frequency region between 600 and 750 cm^{-1}.[37–39]

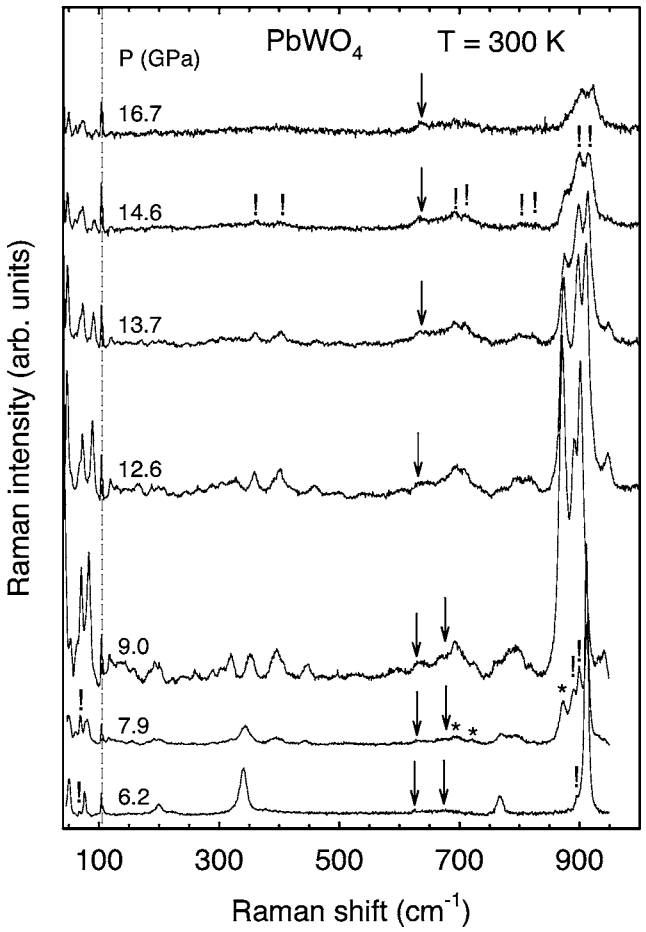

FIG. 4. RT Raman spectra of $PbWO_4$ at different pressures between 6 and 17 GPa. The exclamation marks indicate the Raman peaks assigned to the $PbWO_4$-III phase. The asterisks indicate the Raman peaks assigned to the fergusonite phase. The arrows indicate the position of the silicon-oil modes at different pressures. The dashed line indicates the position of a plasma line of Ar^+ at 104 cm^{-1} used for the calibration of Raman spectra.

B. High-pressure phases

Figure 4 shows the Raman spectra of the high-pressure phases of $PbWO_4$ at different pressures ranging from 6.2 to 17 GPa. At 6.2 GPa many Raman modes of the scheelite phase can still be observed together with new peaks that do not correspond to the scheelite phase (see the exclamation marks in Fig. 4). Therefore, we have taken this value as the pressure of the onset of the first phase transition (see the dotted line in Fig. 3). Apart from the new peaks appearing at 6.2 GPa, there are new Raman peaks appearing at 7.9 GPa (see the asterisks in Fig. 4). In the following we will show that this pressure marks the onset of the second phase transition (see also the dotted line in Fig. 3). The Raman modes of these two new phases coexist with those of the scheelite phase up to 9.0 GPa since the strongest peak of the scheelite phase [$\nu_1(A_g)$ mode] is observed up to this pressure as a high-frequency shoulder of other high-frequency peaks. We must note that on decreasing pressure from 17 GPa the scheelite phase of $PbWO_4$ was recovered below 5 GPa.

The Raman spectra of $PbWO_4$ above 7.9 GPa are completely different from that of the scheelite phase, and are

dominated by three high-frequency peaks located just at lower frequencies than that of the scheelite $\nu_1(A_g)$ mode. The most striking features of the spectrum at 9.0 GPa are (1) the large number of modes observed, which is even larger than the number expected for the fergusonite phase, as we discuss below; (2) some of the new modes are located in the phonon gap of the scheelite phase between 400 and 750 cm^{-1}; (3) the appearance of three modes near the scheelite $\nu_1(A_g)$ mode; (4) the splitting of the scheelite ν_3 modes between 700 and 800 cm^{-1}; and (5) the appearance of several well-separated broad modes between 300 and 500 cm^{-1}.

In the following discussion we will show that the new Raman peaks appearing at 6.2 GPa correspond to the $PbWO_4$-III phase, while the new Raman modes appearing at 7.9 GPa correspond to the fergusonite phase. We will show that, similarly to $BaWO_4$,[10] $PbWO_4$ suffers a scheelite-to-fergusonite and a scheelite-to-$P2_1/n$ phase transition, and that there is a region of coexistence of the scheelite, fergusonite, and $P2_1/n$ phases. Following the method used for $BaWO_4$,[10] the assignment of the Raman modes appearing above 6.2 GPa to the fergusonite and $PbWO_4$-III phases is based on the classification of these modes into two types of modes: (1) modes that appear above 6.2 GPa and decrease in intensity above 10 GPa, but can be followed in pressure up to almost 14.6 or 16.7 GPa; (2) modes that appear above 7.9 GPa that attain a maximum intensity around 9.0 GPa, and weaken more rapidly than the first ones above 10 GPa disappearing above 14 GPa. The different pressure behavior of these two types of modes leads us to believe that between 7.9 and 9.0 GPa we have a mixture of two high-pressure phases with the scheelite one and that between 9.0 and 14 GPa we have a coexistence of the two high-pressure phases. The assignment of the different Raman modes to the two high-pressure phases was difficult because the high-pressure Raman spectra of $PbWO_4$ above 6.2 GPa are considerably different from those reported for the alkaline-earth tungstates.[8,10,26,27] Fortunately, the high-frequency region of the Raman spectrum of $PbWO_4$ between 7.9 and 9.0 GPa resembles that of the Raman spectrum of $BaWO_4$ between 7.5 and 9.0 GPa;[10] so the different pressure behavior of the two types of new modes can be clearly seen in the three strong high-frequency stretching modes appearing in the Raman spectra between 850 and 950 cm^{-1} above 7.9 GPa (see Fig. 4), as it was already observed in $BaWO_4$.[10] In the spectrum at 7.9 GPa there are four strong high-frequency modes. The mode with the highest frequency and intensity at 7.9 GPa is the scheelite $\nu_1(A_g)$ mode, which is observed up to 9 GPa. However, above 9 GPa there are only three intense high-frequency modes that, in light of their similar intensity, we think they derive from the scheelite $\nu_1(A_g)$ mode.[10] The mode with the lowest frequency around 870 cm^{-1} at 9 GPa decreases very rapidly in intensity with increasing pressure, whereas the other two high-frequency modes near 890 cm^{-1} at 9 GPa decrease more slowly in intensity and remain clearly visible up to the highest pressure attained in our experiment. Therefore, in light of the unstability of the fergusonite structure versus the $PbWO_4$-III structure suggested by *ab initio* calculations,[12] we attribute the strong mode near 870 cm^{-1} to the fergusonite phase while the other two strong modes are assigned to the $PbWO_4$-III phase. A decrease in intensity above 10 GPa can also be observed in other modes like the two fergusonite modes with lower frequencies near 40 and 50 cm^{-1} (see the asterisks in Fig. 4). In Secs. IV B 1 and IV B 2 we will discuss more deeply the nature of the different modes assigned to the high-pressure phases.

1. Fergusonite structure

In Ref. 10 it was noted that the Raman modes in $CaWO_4$ and $SrWO_4$ reported between 12 and 20 GPa[26,27] and the Raman modes in $BaWO_4$ appearing at 7.5 GPa and disappearing at 9 GPa[10] correspond to the fergusonite phase. Besides, there is evidence of an experimental scheelite-to-fergusonite phase transition in $PbWO_4$.[12] Therefore, let us begin the study of the Raman peaks of the high-pressure phases in $PbWO_4$ by comparing the expected fergusonite modes with those reported previously.[10,26,27] The centrosymmetric fergusonite structure ($I2/a$, SG No. 15, $Z=4$) should have 36 vibrational modes at the zone center,[10] with the following mechanical representation:

$$\Gamma = 8A_g + 8A_u + 10B_g + 10B_u. \quad (4)$$

The 18 gerade (g) modes are Raman active and the 18 ungerade (u) modes are IR active. The 18 Raman active modes derive from the reduction of the tetragonal C_{4h} symmetry of the scheelite structure to the monoclinic C_{2h} symmetry of the fergusonite structure. In particular, every A_g and every B_g scheelite mode transforms into an A_g mode of the monoclinic symmetry, while every doubly degenerate E_g scheelite mode transforms into two B_g modes of the monoclinic symmetry. Likewise to $BaWO_4$,[10] many Raman modes of scheelite $PbWO_4$ have weakened considerably or disappeared at 9.0 GPa and the number of new modes measured at 9.0 GPa exceed the number of modes expected for the fergusonite structure. These results point out that either the high-pressure phase of $PbWO_4$ is not fergusonite or that there is a mixture of phases with one phase being fergusonite, as evidenced by ADXRD measurements.[12] The above classification of the two classes of Raman modes appearing above 6.2 and 7.9 GPa in $PbWO_4$ makes clear that there is a mixture of phases between 7.9 and 14 GPa. Therefore, taking into account first of all that recent ADXRD measurements observed a fergusonite phase above 9 GPa in $PbWO_4$,[12] that the results of *ab initio* total-energy calculations showed the larger stability of the $PbWO_4$-III phase with respect to the fergusonite phase at high pressures,[12] and finally, that the number of modes appearing at 7.9 GPa and disappearing near 13 GPa is around sixteen, we attribute the modes that appear above 7.9 GPa and disappear progressively above 10 GPa to the fergusonite structure in $PbWO_4$.

Figures 5–7 show enlarged portions of the high-pressure Raman spectra of $PbWO_4$ for a detailed analysis of the behavior of this compound under pressure. The Raman modes assigned to the fergusonite phase are marked with asterisks and the calculated frequencies of the eighteen fergusonite Raman modes at 9 GPa are indicated at the bottom of the figures. In these figures, the appearance of the modes assigned to the fergusonite phase at 7.9 GPa and their fading beginning at 10 GPa can be seen more clearly than in Fig. 4. Figure 3 shows the pressure dependence of the frequencies

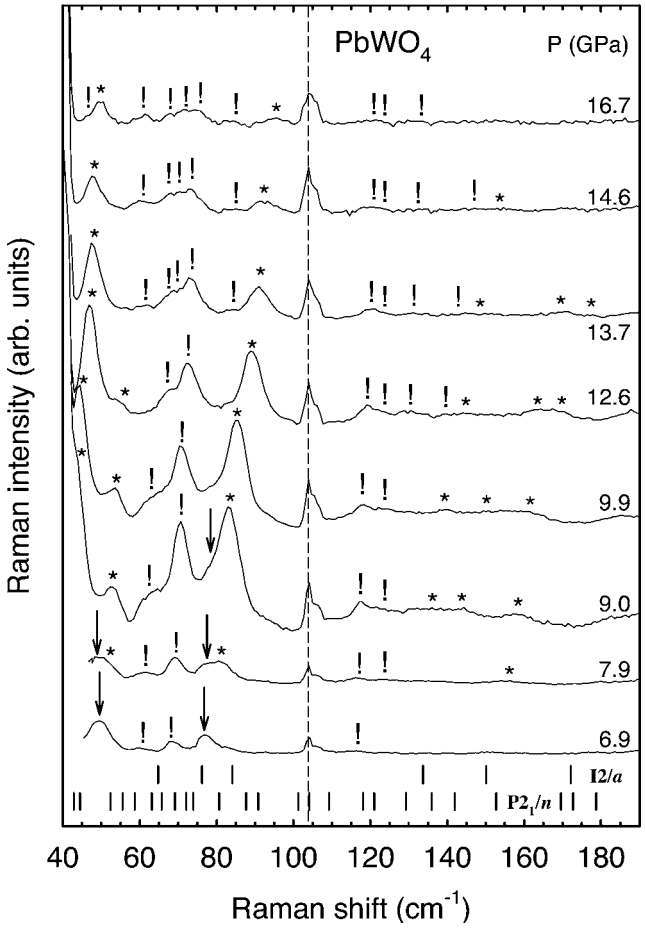

FIG. 5. Detail of the Raman spectra of the fergusonite and $PbWO_4$-III phases of $PbWO_4$ at different pressures at low frequencies. The dashed line indicates the position of a plasma line of Ar^+ at 104 cm^{-1} used for the calibration of Raman spectra. The arrows indicate the position of scheelite modes. The exclamation marks indicate the Raman peaks assigned to the $PbWO_4$-III phase. The asterisks indicate the Raman peaks assigned to the fergusonite phase.

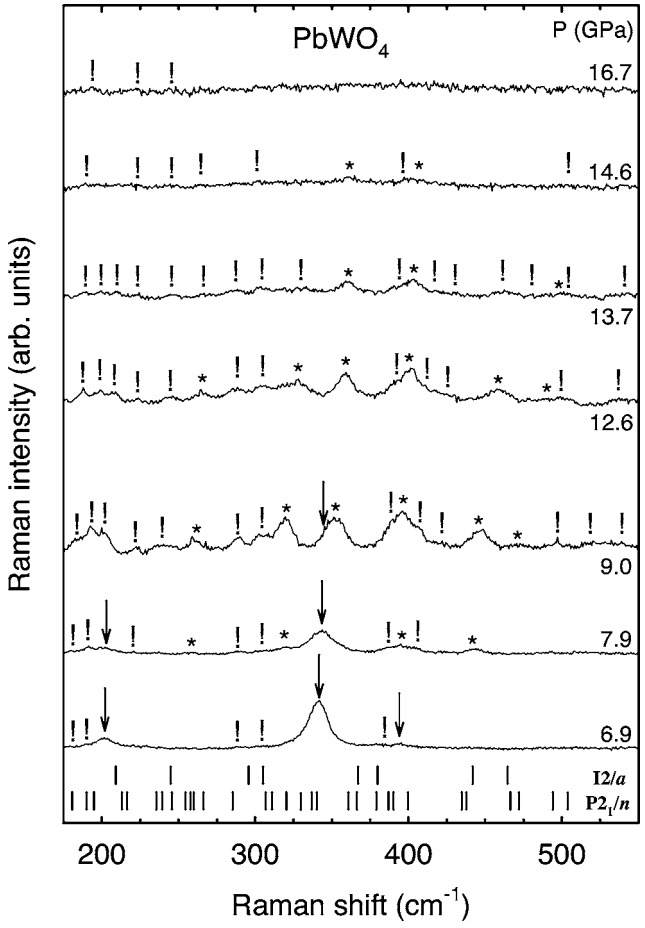

FIG. 6. Detail of the Raman spectra of the fergusonite and $PbWO_4$-III phases of $PbWO_4$ at different pressures at medium frequencies. Arrows indicate the position of scheelite modes. The exclamation marks indicate the Raman peaks assigned to the $PbWO_4$-III phase. The asterisks indicate the Raman peaks assigned to the fergusonite phase.

of the fergusonite Raman modes (empty squares) in $PbWO_4$. Table III summarizes the experimental and theoretical Raman frequencies, and their pressure coefficients for the fergusonite modes at 9 GPa. For completeness, we also report in Table IV the frequencies and pressure coefficients of the calculated IR active modes of fergusonite $PbWO_4$ at 9 GPa. A major conclusion drawn from our calculations and seen in Figs. 6 and 7 is that there is a phonon gap between 470 and 700 cm^{-1} in fergusonite $PbWO_4$ similar to the one observed in scheelite $PbWO_4$. This result is similar to that found in $BaWO_4$ (Ref. 10) and confirms that the fergusonite phase retains at least partially the tetrahedral W coordination of the scheelite phase (see the discussion in Sec. C). It also leads us to conclude that the Raman modes observed at high pressures in this phonon gap belong to a phase other than the scheelite or the fergusonite.

It is difficult to determine the frequency and symmetry of all the modes in the high-pressure phases because the small difference in the rate of intensity decrease between the Raman modes of the fergusonite and $PbWO_4$-III phases makes difficult the assignment of some modes to either of both structures. For the identification of the fergusonite Raman modes in $PbWO_4$ we can make use of the similarities between the scheelite and fergusonite structures already noted in Ref. 10, and the aid of our lattice dynamics calculations. As already commented, the most clear fergusonite mode is the mode located at 870 cm^{-1} at 9 GPa and corresponding to the highest stretching A_g mode arising from the scheelite $\nu_1(A_g)$ mode. Calculations at 9 GPa locate this mode around 846 cm^{-1}; i.e., with an error smaller than 3%, and clearly at smaller frequencies than the other two strong Raman peaks. A striking difference between the scheelite-to-fergusonite phase transitions in $PbWO_4$ and alkaline-earth tungstates is the strong decrease in frequency between the scheelite $\nu_1(A_g)$ mode and the related fergusonite A_g mode in $PbWO_4$ (40 cm^{-1}), as compared to the slight change in frequency observed in the alkaline-earth tungstates (5 cm^{-1}).[10,26,27] Curiously enough, the jump observed in $PbWO_4$ seems not to occur in $PbMoO_4$ according to the frequencies reported in Ref. 9. We will comment on this fact in Sec. IV C when discussing the W coordination in the high-pressure phases. The other three high-frequency stretching fergusonite modes

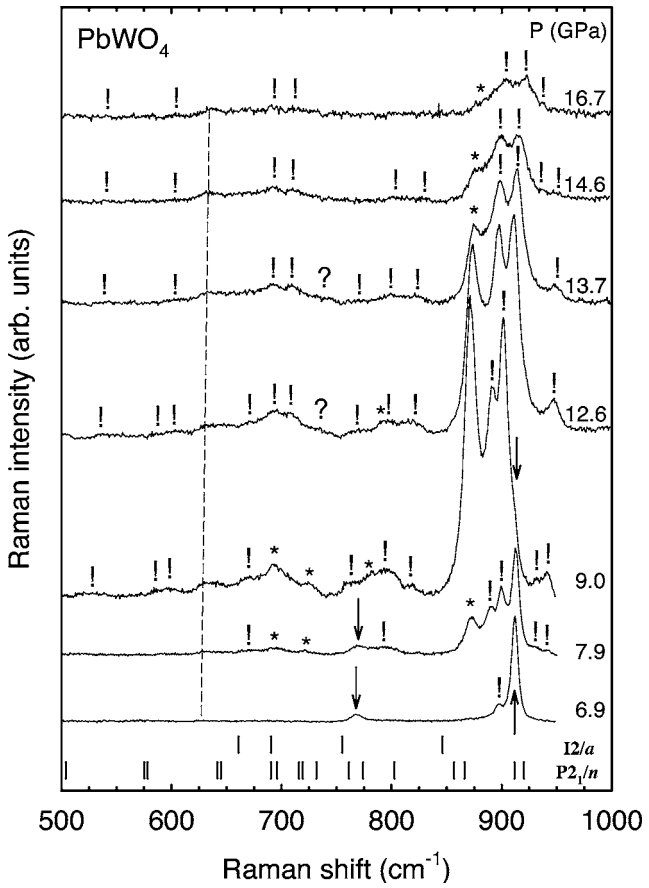

FIG. 7. Detail of the Raman spectra of the fergusonite and $PbWO_4$-III phases of $PbWO_4$ at different pressures at high frequencies. The arrows indicate the position of scheelite modes. The asterisks indicate the position of fergusonite modes. The exclamation marks indicate the Raman peaks assigned to the $PbWO_4$-III phase. Asterisks indicate the Raman peaks assigned to the fergusonite phase. The dashed line indicates the position of one of the silicon-oil modes observed at high pressures.

can be located and assigned with the aid of their calculated frequencies (also slightly underestimated) and pressure coefficients, and due to its larger intensity in the Raman spectrum at 9 GPa (see Fig. 7 and Table III). Note that the fergusonite phase is dominant in the Raman spectrum of $PbWO_4$ at 9 GPa in agreement with ADXRD measurements.[12]

Concerning the five fergusonite modes arising from the four scheelite ν_2 and ν_4 modes, we have tentatively assigned the 446 and 471 cm^{-1} experimental peaks to the two fergusonite B_g modes arising from the scheelite $\nu_4(E_g)$ mode. Support for this assignment is given by the closeness of the calculated modes (440 and 467 cm^{-1} at 9 GPa) and by the qualitative agreement between the large pressure coefficients measured and calculated for these two modes (see Table III). In Sec. IV C we will discuss why the pressure coefficients of these two fergusonite modes are considerably larger than those of other fergusonite modes. The mode measured at 396 cm^{-1} at 9 GPa has been identified as the fergusonite A_g mode arising from the scheelite $\nu_4(A_g)$ mode with a calculated frequency of 377 cm^{-1} at 9 GPa. And finally, the two

TABLE III. Frequencies and pressure coefficients of the Raman modes in fergusonite $PbWO_4$ at 9 GPa. The fergusonite frequencies and pressure coefficients obtained after *ab initio* calculations at 9 GPa are also given for comparison.

Peak/mode	$\omega(9)$ cm^{-1}	$d\omega/dP$ cm^{-1}/GPa	$\omega(9)^a$ cm^{-1}	$d\omega/dP^a$ cm^{-1}/GPa
$F1$ (B_g)	44(1)	0.8(1)	65	1.9
$F2$ (A_g)	53(1)	0.4(2)	78	1.5
$F3$ (B_g)	85(1)	1.4(3)	84	1.6
$F4$ (B_g)	136(1)	3.7(3)	134	4.2
$F5$ (A_g)	144(1)	5.5(5)	150	5.0
$F6$ (B_g)	158(1)	4.0(1)	173	3.6
$F7$ (B_g)			206	7.5
$F8$ (B_g)			247	7.0
$F9$ (A_g)	261(1)	1.9(1)	295	3.7
$F10$ $\nu_2(A_g)$	320(1)	1.9(3)	303	4.0
$F11$ $\nu_2(A_g)$	352(1)	1.7(2)	365	3.2
$F12$ $\nu_4(A_g)$	396(1)	0.9(1)	377	2.5
$F13$ $\nu_4(B_g)$	446(1)	3.2(2)	440	5.4
$F14$ $\nu_4(B_g)$	471(1)	5.6(5)	467	7.9
$F15$ $\nu_3(A_g)$	693(1)	1.0(2)	661	6.8
$F16$ $\nu_3(B_g)$	725(2)	3.3(4)	689	−0.8
$F17$ $\nu_3(B_g)$	779(1)	3.6(5)	752	4.4
$F18$ $\nu_1(A_g)$	872(1)	0.9(1)	846	1.0

[a]*Ab initio* calculations.

modes located at 320 and 352 cm^{-1} at 9 GPa have been assigned to the fergusonite A_g modes arising from the scheelite ν_2 modes with calculated frequencies of 303 and 365 cm^{-1} at 9 GPa. The three above assignments are supported also by the qualitative agreement between the measured and calculated pressure coefficients. We should note that even though the measured pressure coefficients are smaller than the calculated ones for the fergusonite modes, in general the qualitative agreement guiding our assignments is good (see Table III).

In regard to the external fergusonite modes in $PbWO_4$, first of all we have to note that contrary to what happens in scheelite alkaline-earth tungstates, the translational (T) modes in stolzite are well separated in frequency from the rotational (R) modes. Therefore, we expect six fergusonite Raman modes below 200 cm^{-1} arising from the four T scheelite modes plus three fergusonite Raman modes above 200 cm^{-1} arising from the two R scheelite modes, as indeed observed from our calculations (see Figs. 5 and 6). However, like in alkaline-earth tungstates,[10] we have not found experimentally the two fergusonite modes coming from the scheelite $R(E_g)$ mode in $PbWO_4$. We believe that their absence can be due to the weak intensity of these two modes already in the scheelite phase. Furthermore, these two fergusonite modes have very large calculated pressure coefficients that do not agree with any of our observed modes. However, we think that we have experimentally found the fergusonite A_g mode deriving from the scheelite $R(A_g)$ mode near 250 cm^{-1} at 9 GPa on the basis of the measured and calculated frequency and pressure coefficient.

TABLE IV. IR mode frequencies and pressure coefficients in fergusonite $PbWO_4$ obtained from *ab initio* calculations at 9 GPa.

Peak/mode	$\omega(9)$ cm^{-1}	$d\omega/dP$ cm^{-1}/GPa
$F1$ (A_u)	0	
$F2$ (B_u)	0	
$F3$ (B_u)	0	
$F4$ (A_u)	85	2.9
$F5$ (B_u)	91	1.2
$F6$ (B_u)	114	3.4
$F7$ (A_u)	161	6.8
$F8$ (B_u)	210	6.9
$F9$ (B_u)	215	1.3
$F10$ (A_u)	295	3.1
$F11$ (A_u)	306	7.8
$F12$ (A_u)	356	9.1
$F13$ (B_u)	388	2.7
$F14$ (B_u)	463	7.6
$F15$ (B_u)	610	2.9
$F16$ (B_u)	705	2.2
$F17$ (A_u)	720	3.5
$F18$ (A_u)	854	6.1

In order to identify the fergusonite modes arising from the scheelite T modes, we will begin discussing those with smaller frequencies. There are two modes with frequencies near 44 and 53 cm^{-1} at 9 GPa (see the asterisks in Fig. 5) whose intensities decrease strongly above 10 GPa. We have tentatively attributed the mode at 53 cm^{-1} to the lowermost fergusonite A_g mode arising from the lowermost scheelite $T(B_g)$ mode. On the other hand, we have attributed the mode at 44 cm^{-1} to the lowermost fergusonite B_g mode arising from the lowermost scheelite $T(E_g)$ mode. The other fergusonite B_g mode arising from this scheelite T mode is located around 63 cm^{-1} in agreement with *ab initio* calculations. The present assignment for the two lowermost fergusonite modes is supported by the small pressure coefficient of the fergusonite mode derived from the soft scheelite $T(B_g)$ mode with negative pressure coefficient. However, the calculated fergusonite frequencies for these two modes are considerably higher than the experimentally observed modes (see Table III). A similar overestimation of the experimental frequencies was also found for the external modes with the smallest frequencies in fergusonite $BaWO_4$.[10] It is curious that, unlike $BaWO_4$, the fergusonite mode arising from the soft scheelite $T(B_g)$ mode in $PbWO_4$ does not exhibit a negative pressure coefficient (0.4 cm^{-1}/GPa). We think that this could be due to the strong deformation of the WO_4 tetrahedra in the fergusonite phase of $PbWO_4$, which is shown by *ab initio* total-energy calculations[12] and will be discussed in Sec. IV C. The deformation of the fergusonite structure in $PbWO_4$ makes this structure more stable in $PbWO_4$ than in $BaWO_4$, where the instability of this phase was evidenced by the quick disappearance of its Raman modes above 8.2 GPa.[10] In contrast, Raman modes of fergusonite $PbWO_4$ last almost up to 14.6 GPa. Finally, there are three calculated fergusonite modes between 100 and 200 cm^{-1} arising from the topmost T modes with similar pressure coefficients to those measured for the three experimental modes at 136, 144, and 152 cm^{-1}. The agreement between the experimental and the theoretical frequencies and pressure coefficients justifies the above assignments (see Table III).

2. $PbWO_4$-III *structure*

The existence of a high-pressure structure in $PbWO_4$ having the $PbWO_4$-III structure[7] has been recently suggested by Errandonea *et al.*[12] The experimental powder ADXRD patterns above 15 GPa are compatible with the $PbWO_4$-III structure.[12] In this section, we will show with the help of our *ab initio* lattice-dynamics calculations that the Raman modes of $PbWO_4$ appearing above 6.2 GPa; i.e., before the appearance of modes corresponding to the fergusonite phase at 7.9 GPa, are consistent with the *ab initio* total-energy calculations, which yield a lower value (5.3 GPa) for the scheelite/$PbWO_4$-III coexistence pressure than for the scheelite/fergusonite one (8 GPa).[12] This result leads us to attribute the new Raman modes appearing at 6.2 GPa and lasting up to 17 GPa to the $PbWO_4$-III phase (see the exclamation marks in Figs. 5–7). This phase shows a distorted octahedral W-O coordination, which can explain the Raman modes observed above 6.2 GPa in the phonon gap of the scheelite and fergusonite phases. Similar modes have also been observed in $BaWO_4$ above 6.9 GPa[10] and in $BaMoO_4$ above 9 GPa.[40,41]

The centrosymmetric $PbWO_4$-III structure is isomorphous to the $BaWO_4$-II structure ($P2_1/n$, SG No. 14, $Z=8$)[7,10] and group theoretical considerations lead to the following mechanical representation of vibrational modes at Γ:[21]

$$\Gamma = 36A_g + 36A_u + 36B_g + 36B_u. \quad (5)$$

There are 72 Raman active (g) modes and 72 IR active (u) modes, of which one A_u and two B_u are the acoustic modes. One thus expects four times more Raman modes in the $PbWO_4$-III phase than in the fergusonite phase. The experimental assignment of the mode symmetry in the $PbWO_4$-III phase is difficult because of its mixture with the fergusonite phase, because of the impossibility of testing the polarization selection rules of the Raman modes inside the DAC, and because the number of modes that can be clearly resolved in the experimental Raman spectra above 6.2 GPa is around 37; i.e., about half the number of expected modes for the $PbWO_4$-III phase.

In Ref. 10 we listed a number of factors that can explain why a large number of modes of the $BaWO_4$-II ($PbWO_4$-III) structure are not observed experimentally. In any case, the observation of most of the *ab initio*-predicted modes for the $PbWO_4$-III phase in certain frequency ranges, especially in the phonon gap of the scheelite and fergusonite phases, evidences that there is no other structure with higher symmetry, such as $LaTaO_4$ ($P2_1/c$, SG No. 14, $Z=4$) or raspite with half the number of expected modes than the $PbWO_4$-III phase, which could account for the experimentally observed modes.

TABLE V. Frequencies and pressure coefficients of the Raman modes observed in the $PbWO_4$-III phase at 13.7 GPa.

Peak/mode	$\omega(13.7)$ cm^{-1}	$d\omega/dP$ cm^{-1}/GPa	Peak/mode	$\omega(13.7)$ cm^{-1}	$d\omega/dP$ cm^{-1}/GPa
*P*1	46(1)		*P*20	400(1)	
*P*2	61(1)	0.2(2)	*P*21	417(2)	2.1(3)
*P*3	68(1)	0.0(2)	*P*22	430(1)	2.2(2)
*P*4	69(1)	1.2(2)	*P*23	490(3)	1.1(3)
*P*5	73(1)	0.7(1)	*P*24	501(2)	1.1(2)
*P*6	84(1)	0.0(2)	*P*25	542(2)	4.6(5)
*P*7	120(1)	0.6(1)	*P*26	564(3)	5.4(6)
*P*8	123(1)	0.0(2)	*P*27	605(3)	1.6(2)
*P*9	130(2)	0.6(1)	*P*28	672(3)	0.2(1)
*P*10	145(2)	4.5(9)	*P*29	693(2)	0.7(1)
*P*11	189(1)	0.9(2)	*P*30	710(2)	1.0(2)
*P*12	201(1)	1.2(2)	*P*31	773(2)	1.6(2)
*P*13	208(1)	1.3(2)	*P*32	799(2)	1.4(2)
*P*14	222(5)	0.2(2)	*P*33	825(3)	1.9(3)
*P*15	246(1)	1.3(3)	*P*34	899(1)	1.5(3)
*P*16	266(1)	–2.2(5)	*P*35	914(1)	2.5(3)
*P*17	288(1)	0.0(3)	*P*36	935(2)	0.8(1)
*P*18	305(1)	0.0(3)	*P*37	949(2)	1.5(4)
*P*19	390(1)	0.0(3)			

The pressure dependence of the Raman modes observed experimentally and attributed to the $PbWO_4$-III phase is shown in Fig. 3 with solid triangles. The experimentally observed frequencies and pressure coefficients of the Raman modes attributed to the $PbWO_4$-III phase at 13.7 GPa are summarized in Table V. The assignment of the modes corresponding to the $PbWO_4$-III has been done with the help of lattice dynamics calculations for this phase at 9 GPa. Tables VI and VII summarize the calculated frequencies and symmetries of the Raman and IR modes attributed to the $PbWO_4$-III phase at 9 GPa, respectively. The frequencies of the Raman modes of the $PbWO_4$-III phase calculated at 9 GPa are marked at the bottom of Figs. 5–7.

As commented on previously, our assignment of the high-pressure phase of $PbWO_4$, stable between 6.2 and 17 GPa, to the $PbWO_4$-III phase is supported by the observation, in several cases, of the four peaks expected for each fergusonite mode at frequencies close to those obtained from our lattice-dynamics calculations. Clear examples of this fact can be seen in the high-frequency region above 500 cm^{-1}, due to the smaller density of modes in this region. The Raman spectra above 9 GPa show two strong high-frequency modes, located at 899 and 914 cm^{-1} at 13.7 GPa. In addition two weak high-frequency modes, located at 935 and 949 cm^{-1} at 13.7 GPa, appear as shoulders rather than as full peaks (see the exclamation marks in Fig. 7). *Ab initio* calculations for the $PbWO_4$-III phase at 9 GPa show that many modes in this phase are grouped in pairs (see the marks at the bottom of Figs. 5–7). In particular, there are two groups of high-frequency modes located around 860 and 910 cm^{-1} at 9 GPa. We attribute these four modes to phonons in the $PbWO_4$-III phase that likely arise from the splitting of the scheelite $\nu_1(A_g)$ mode or its related fergusonite A_g mode despite the fact that the calculated frequencies are around 30 cm^{-1} (4%) below our experimentally observed modes. This is the clear-

TABLE VI. Raman mode symmetries and frequencies in the $PbWO_4$-III phase as obtained from *ab initio* calculations at 8.7 GPa.

Mode (symmetry)	$\omega(8.7)$ (cm^{-1})	Mode (symmetry)	$\omega(8.7)$ (cm^{-1})	Mode (symmetry)	$\omega(8.7)$ (cm^{-1})	Mode (symmetry)	$\omega(8.7)$ (cm^{-1})
*R*1 (B_g)	43	*R*19 (A_g)	130	*R*37 (A_g)	269	*R*55 (A_g)	495
*R*2 (A_g)	44	*R*20 (B_g)	136	*R*38 (B_g)	283	*R*56 (B_g)	503
*R*3 (B_g)	52	*R*21 (B_g)	142	*R*39 (B_g)	306	*R*57 (A_g)	575
*R*4 (A_g)	56	*R*22 (A_g)	153	*R*40 (A_g)	309	*R*58 (B_g)	576
*R*5 (A_g)	59	*R*23 (B_g)	170	*R*41 (A_g)	321	*R*59 (A_g)	644
*R*6 (A_g)	63	*R*24 (A_g)	171	*R*42 (B_g)	332	*R*60 (B_g)	645
*R*7 (B_g)	66	*R*25 (A_g)	173	*R*43 (A_g)	340	*R*61 (A_g)	694
*R*8 (B_g)	69	*R*26 (B_g)	179	*R*44 (B_g)	341	*R*62 (B_g)	697
*R*9 (A_g)	72	*R*27 (A_g)	191	*R*45 (B_g)	362	*R*63 (B_g)	718
*R*10 (A_g)	74	*R*28 (B_g)	196	*R*46 (A_g)	368	*R*64 (A_g)	719
*R*11 (B_g)	81	*R*29 (B_g)	213	*R*47 (A_g)	380	*R*65 (A_g)	730
*R*12 (A_g)	87	*R*30 (A_g)	215	*R*48 (B_g)	390	*R*66 (B_g)	761
*R*13 (B_g)	91	*R*31 (B_g)	232	*R*49 (A_g)	391	*R*67 (A_g)	774
*R*14 (B_g)	101	*R*32 (B_g)	237	*R*50 (B_g)	400	*R*68 (B_g)	802
*R*15 (A_g)	104	*R*33 (A_g)	244	*R*51 (B_g)	436	*R*69 (A_g)	857
*R*16 (B_g)	109	*R*34 (A_g)	255	*R*52 (A_g)	438	*R*70 (B_g)	869
*R*17 (A_g)	118	*R*35 (B_g)	258	*R*53 (A_g)	467	*R*71 (A_g)	912
*R*18 (B_g)	121	*R*36 (A_g)	259	*R*54 (B_g)	472	*R*72 (B_g)	919

TABLE VII. IR mode symmetries and frequencies in the $PbWO_4$-III phase as obtained from *ab initio* calculations at 8.7 GPa.

Mode (symmetry)	ω(8.7) (cm^{-1})	Mode (symmetry)	ω(8.7) (cm^{-1})	Mode (symmetry)	ω(8.7) (cm^{-1})	Mode (symmetry)	ω(8.7) (cm^{-1})
$I1$ (A_u)	0	$I19$ (A_u)	105	$I37$ (B_u)	283	$I55$ (A_u)	442
$I2$ (B_u)	0	$I20$ (A_u)	118	$I38$ (A_u)	284	$I56$ (B_u)	447
$I3$ (B_u)	0	$I21$ (A_u)	135	$I39$ (B_u)	296	$I57$ (A_u)	543
$I4$ (B_u)	36	$I22$ (B_u)	140	$I40$ (A_u)	302	$I58$ (B_u)	548
$I5$ (A_u)	38	$I23$ (B_u)	147	$I41$ (A_u)	317	$I59$ (B_u)	605
$I6$ (A_u)	47	$I24$ (A_u)	148	$I42$ (B_u)	322	$I60$ (A_u)	606
$I7$ (B_u)	61	$I25$ (A_u)	177	$I43$ (B_u)	328	$I61$ (A_u)	705
$I8$ (B_u)	61	$I26$ (B_u)	178	$I44$ (A_u)	338	$I62$ (B_u)	706
$I9$ (A_u)	62	$I27$ (A_u)	183	$I45$ (A_u)	359	$I63$ (A_u)	720
$I10$ (B_u)	69	$I28$ (B_u)	185	$I46$ (B_u)	361	$I64$ (B_u)	727
$I11$ (A_u)	70	$I29$ (B_u)	202	$I47$ (B_u)	374	$I65$ (B_u)	742
$I12$ (A_u)	72	$I30$ (A_u)	213	$I48$ (A_u)	380	$I66$ (A_u)	778
$I13$ (B_u)	77	$I31$ (A_u)	220	$I49$ (B_u)	388	$I67$ (A_u)	779
$I14$ (B_u)	84	$I32$ (B_u)	228	$I50$ (A_u)	392	$I68$ (B_u)	804
$I15$ (A_u)	92	$I33$ (A_u)	245	$I51$ (A_u)	397	$I69$ (B_u)	862
$I16$ (B_u)	94	$I34$ (B_u)	248	$I52$ (B_u)	400	$I70$ (A_u)	864
$I17$ (A_u)	98	$I35$ (B_u)	259	$I53$ (B_u)	418	$I71$ (B_u)	898
$I18$ (B_u)	104	$I36$ (A_u)	273	$I54$ (A_u)	438	$I72$ (A_u)	911

est example we have found of the observation of four modes in the $PbWO_4$-III phase for every fergusonite mode, supporting the $PbWO_4$-III nature of the high-pressure phase.

Ab initio calculations show four fergusonite modes and sixteen $PbWO_4$-III modes above 550 cm^{-1} (see Fig. 7), in agreement with the 4:1 $PbWO_4$-III/fergusonite mode ratio commented on previously. Therefore, we think that many of the Raman modes of the $PbWO_4$-III phase can be reasonably identified at least in the high-frequency region with a smaller density of Raman peaks. In this sense, the two modes of the calculated pairs can be experimentally observed in many cases above 500 cm^{-1}. For instance, there are two pairs of calculated modes around 500 and another two around 575 cm^{-1} at 9 GPa (see the marks at the bottom of Figs. 6 and 7). One can distinguish these two pairs of modes between 520 and 540 cm^{-1} and between 575 and 600 cm^{-1} at 9 GPa (see the exclamation marks in Figs. 6 and 7). In a similar way, there is a pair of calculated modes near 640 cm^{-1} that can be correlated to the broadband located 670 cm^{-1} at 9 GPa. Furthermore, we believe that the two modes observed at 693 and 710 cm^{-1} at 13.7 GPa correspond to the calculated pair located near 690 cm^{-1} at 9 GPa, and that the three calculated modes around 925 cm^{-1} at 9 GPa cannot be clearly observed but contribute to the broadband marked with a question mark in the Raman spectra of Fig. 7 above 12.6 GPa. Finally, we tentatively attribute the modes located at 762, 790, and 820 cm^{-1} at 9 GPa to those calculated at 761, 774, and 802 cm^{-1} at 9 GPa. All the above examples give evidence that the $PbWO_4$-III phase can be reasonably identified, despite the number of Raman modes distinguished in the experimental spectra at high pressures is well below the number of expected modes for this phase. We are not going to discuss the correlation between experimentally observed and calculated modes of the $PbWO_4$-III phase in the low-frequency region because it is much more complicated due to the overlapping of modes in this region with a higher density of Raman modes.

Finally, we should mention that the coexistence of the scheelite, fergusonite, and $PbWO_4$-III phases is possible due to the kinetic hindrance of the reconstructive scheelite-to-$PbWO_4$-III transition and the displacive second-order nature of the scheelite-to-fergusonite transition.[42] This is the same case as in $BaWO_4$.[10] The kinetic hindrance of the scheelite-to-$PbWO_4$-III transition can be clearly observed in our Raman spectra between 6.9 and 10 GPa by checking the intensity of the two strong high-frequency peaks attributed to the $PbWO_4$-III phase and located at 899 and 914 cm^{-1} at 13.7 GPa. The low-frequency mode of this pair grows in intensity between 9 and 12.6 GPa becoming as intense as the high-frequency mode of this pair only at 14.6 GPa. Besides, it can be observed as an overall change in the Raman spectrum between 9 and 12.6 GPa showing a decrease in intensity in many fergusonite modes and the appearance of some new modes at 12.6 and 13.7 GPa. All these results indicate that the scheelite-to-$PbWO_4$-III phase transition is not completed up to 14.6 GPa (see the dashed line in Fig. 3). This is in good agreement with the results of ADXRD and XANES that showed a different phase from fergusonite above 15.6 and 16.7 GPa, respectively.[12] We believe that the Raman spectrum above 13.7 GPa corresponds mainly to the $PbWO_4$-III phase with the stretching fergusonite A_g mode testifying to the presence of a vanishing fergusonite phase (see Fig. 7). The presence of some modes in the $PbWO_4$-III phase with a zero or even negative pressure coefficient,

the overall decrease in intensity of the spectrum above 14.6 GPa, and the lack of good ADXRD spectra even at 10 GPa,[12] lead us to suspect that the $PbWO_4$-III phase is not very stable and could tend to another phase or to amorphization above 17 GPa. However, on the downstroke from 17 GPa the appearance of the strongest Raman peak of the scheelite phase below 5 GPa after a considerable hysteresis indicates that the scheelite-to-fergusonite and scheelite-to-$PbWO_4$-III phase transitions are reversible, as in the case of $BaWO_4$.[10] This result is in agreement with Refs. 9 and 12.

In summary, we can conclude that the onset of the scheelite-to-$PbWO_4$-III phase transition is found around 6.2 GPa, being followed by a scheelite-to-fergusonite phase transition around 7.9 GPa. These phase-transition pressures are in excellent agreement with the pressure of the scheelite-to-$PbWO_4$-III transition (5.3 GPa) and the pressure of the scheelite-to-fergusonite transition (8.0 GPa) found recently by *ab initio* total-energy calculations.[12] The observation of the coexistence of the scheelite, fergusonite, and $PbWO_4$-III phases between 7.9 and 9.0 GPa, and the coexistence of the fergusonite and $PbWO_4$-III phases up to 14.6 GPa, can only be explained by the kinetic hindrance of the reconstructive scheelite-to-$PbWO_4$-III phase transition that favors the observation of the second-order scheelite-to-fergusonite phase transition, as already discussed in Refs. 10, 12, and 42.

We want to close this section showing that our results for the fergusonite and $PbWO_4$-III phases can also give account for the results of $PbWO_4$ reported up to 9 GPa by Jayaraman *et al.*[9] in the same way as in Sec. IV B 1 we showed that our results for stolzite are consistent with those previously reported.[9] In Ref. 9, the three high-frequency stretching modes arising from the scheelite $\nu_1(A_g)$ mode were observed above 4.5 GPa.[9] As regards to the modes of the $PbWO_4$-III phase, one of the two high-frequency stretching modes assigned to the $PbWO_4$-III structure near 900 cm^{-1} is reported at 4.5 GPa (2.4 GPa below our measurements), and the other one above 6.5 GPa, likely due to their overlapping and limited resolution. Besides, two modes near 300 cm^{-1}, and two modes around 800 cm^{-1} were observed at 4.5 GPa in agreement with our assignment of these modes to the $PbWO_4$-III phase. Regarding the fergusonite modes, the high-frequency A_g stretching mode at 870 cm^{-1} is in fact reported by Jayaraman *et al.* above 6.5 GPa (1.4 GPa below our measurements). The major disagreement between the present and previous works seems to be the assignment of the lowest-frequency mode around 45 cm^{-1}. This mode was previously observed above 4.5 GPa,[9] but we have observed it above 9 GPa. The observation of this mode already at 4.5 GPa would suggest that this mode could correspond to the $PbWO_4$-III phase and not to the fergusonite phase, as we have considered. We cannot rule out the possibility that this mode corresponds to the $PbWO_4$-III phase, given the frequency difference between the measured and calculated fergusonite mode commented on previously, and the fact that our *ab initio* calculations locate two modes of the $PbWO_4$-III phase near 44 cm^{-1} at 9 GPa. Finally, we have to point out that, in our opinion, the Raman spectra of $PbWO_4$ in Ref. 9 agree qualitatively with ours despite the fact that we observe the phase transitions at rather higher pressures than in Ref. 9. Furthermore, we think that the coexistence of the two high-pressure phases is also observed in Ref. 9 between 6.5 and 8.5 GPa.

C. Tungsten coordination in high-pressure phases

Our assignment of the Raman modes in the high-pressure phases to the fergusonite and $PbWO_4$-III phases is coherent with the change of W coordination from tetrahedral to octahedral with increasing pressure. Features that support a basically tetrahedral W coordination in the fergusonite phase and an octahedral W coordination in the $PbWO_4$-III phase are (1) the presence of a phonon gap in the fergusonite phase (between 470 and 700 cm^{-1}) similar to that of the scheelite phase; and (2) the appearance of modes of the $PbWO_4$-III phase in the phonon gap of the scheelite and fergusonite phases. However, the tetrahedral W coordination in the fergusonite phase is not fully compatible with the strong decrease of the highest-frequency stretching A_g mode from 912 cm^{-1} in the scheelite phase to 870 cm^{-1} in the fergusonite phase. This strong decrease in frequency suggests larger W-O distances in the fergusonite phase than in the scheelite phase compatible with an octahedral W coordination in the high-pressure phase. Furthermore, in alkaline-earth tungstates, where the fergusonite phase retains the tetrahedral W coordination of the scheelite phase, there is a very small change in the high-frequency A_g stretching mode at the scheelite-to-fergusonite transition due to the small change of the shorter W-O bond distance between the two phases.[10] In the discussion below we will show that the large decrease of the highest-frequency mode of the fergusonite phase in $PbWO_4$ is clearly due to the tendency of fergusonite $PbWO_4$ to octahedral W coordination.

As previously commented on in Ref. 10, there is a relationship between the frequencies of the stretching W-O modes and the bond distance R (in Å) between W and O in tungsten oxides,[43]

$$\omega(\mathrm{cm}^{-1}) = 25823 \exp(-1.902R) \tag{6}$$

and there is a relationship between the bond distance R (in Å) and the Pauling's bond strength s, which for tungsten oxides is:[44]

$$s_{\mathrm{W\text{-}O}} = (R/1.904)^{-6}, \tag{7}$$

with $s_{\mathrm{W\text{-}O}}$ given in valence units (v.u.) and with 1.904 Å being the bond distance corresponding to the unit valence.

By taking the values of 752, 766, and 906 cm^{-1} as the stretching frequencies of stolzite at 1 atm, we can estimate with Eqs. (6) and (7) three W-O bond distances 1.86, 1.85, and 1.76 Å, and three bond strengths 1.15, 1.19, and 1.59 v.u., respectively. With the three bond strengths we can estimate a total valence of 5.53 v.u., which matches approximately the formal valence of the W^{6+} ion (6).[43] To obtain this result, we must consider a double contribution of the shortest bond distance on the basis of the fourfold W coordination (four W-O distances instead of three) in the scheelite structure.[43] In this configuration, the double contribution of the shorter distance leads to an average W-O distance of 1.808 Å in good agreement with the estimated W-O bond distance from x-ray and neutron-diffraction measure-

ments.[12,15] The above result agrees also with the expected ideal W-O bond distance in tetrahedral *W* coordination (1.78 Å), which corresponds to a Pauling's bond strength of 1.5 v.u. in Eq. (7) for each of the four W-O bonds.[43] However, the rather small value for the total W^{6+} ion valence in stolzite (5.5 v.u.) than in alkaline-earth tungstates (5.8-5-9 v.u.)[10] using empirical data and Eqs. (6) and (7) could suggest a small W-O bond strength in stolzite, responsible for the smaller frequencies of the internal modes of the WO_4 tetrahedron, and consequently a tendency of stolzite to octahedral W coordination. Note that Hg and Pb have similar masses and electronegativities and $HgWO_4$ crystallizes in the $C2/c$ structure where W is octahedrally coordinated.[45]

In a similar way, we can take the values of 872, 779, 725 and 693 cm^{-1} as the stretching frequencies of fergusonite $PbWO_4$ at 9 GPa (see Table III). With these four frequencies we have estimated the W-O bond distances of 1.78, 1.84, 1.88, and 1.90 Å, and the strengths of 1.49, 1.23, 1.1, and 1.0 v.u., respectively. In total they sum 4.8 v.u. for the W ion, i.e., much lower than the formal valence of the W^{6+} ion (6). This result also casts a doubt about the fourfold coordination in fergusonite $PbWO_4$, and suggests a higher W coordination in this phase. If this were the case, additional stretching modes should be considered in the calculations using Eqs. (6) and (7). Taking the next two internal modes in order of decreasing frequency; i.e., those at 471 and 446 cm^{-1} at 9 GPa, as the remaining stretching modes in fergusonite $PbWO_4$, we found that they would correspond to W-O bond distances of 2.10 and 2.13 Å, respectively, according to Eq. (6), and they would yield bond strengths of 0.55 and 0.51 v.u., according to Eq. (7). Therefore, adding these values to the previous results we would get a total sum of 5.86 v.u., which matches nicely the formal valence of the W^{6+} ion. This result clearly indicates that the fergusonite structure in $PbWO_4$ shows a 4+2 coordination for W, and that this is the reason for the strong decrease of the high-frequency A_g stretching mode arising from the scheelite $\nu_1(A_g)$ mode after the scheelite-to-fergusonite phase transition. This strong decrease of the highest stretching frequency must be related to a structural change in the W-O distances in $PbWO_4$ giving a strong distortion of the WO_4 tetrahedra after the scheelite-to-fergusonite transition.

Figure 8 shows *ab initio* calculations of the W-O bond distances in the scheelite and fergusonite phases of $PbWO_4$. Details of these calculations are given in Ref. 12. It can be seen how the two different W-O distances in the scheelite phase change considerably after the phase transition. The four shorter and equal W-O bond distances in the scheelite phase split into two pairs of different and slightly larger distances. On the other hand, the four larger and equal second-neighbor W-O distances in the scheelite phase suffer a big splitting at the phase transition leading to two W-O bond distances around 2.25 Å at 9.5 GPa. This big decrease of second-neighbor W-O distances justify the 4+2 coordination for W in the fergusonite phase of $PbWO_4$. Moreover, the big change of interatomic distances and the distortion of the W-O bonds in fergusonite $PbWO_4$ are evidence that this phase in $PbWO_4$ acts as a bridge phase between a structure with fourfold and another with sixfold W coordination. Furthermore, we should note that the estimated W-O bond distances using Eq. (6) and corresponding to the above six fergusonite stretching Raman modes taken in pairs (1.74+1.84, 1.88+1.90, and 2.10+2.13), give average W-O bond distances of 1.79, 1.89, and 2.12 Å at 9 GPa. These values are reasonably close to those found by *ab initio* calculations in Fig. 8 for the fergusonite structure at 9.5 GPa (1.80, 1.88, and 2.25 Å), and confirm that Eqs. (6) and (7) allow the prediction of the 4+2 coordination for W in the fergusonite structure of $PbWO_4$. Finally, we want to point out that the change of W coordination after the scheelite-to-fergusonite transition in $PbWO_4$ unlike in alkaline-earth tungstates and the sensitivity of XANES to coordination changes allows us to explain why XANES measurements detected the scheelite-to-fergusonite phase transition in $PbWO_4$ around 9 GPa, but not in $BaWO_4$.[12] Furthermore, the change from 4+2 coordination for W in fergusonite $PbWO_4$ to 6 coordination in the $PbWO_4$-III phase allows an explanation of the faint observation of the fergusonite-to-$PbWO_4$-III phase transition in XANES at 16.7 GPa.[12] The lack of a clear transition between the fergusonite and $PbWO_4$-III phases, as found in XANES measurements,[12] is coherent with the large monoclinic distortion of the fergusonite structure in $PbWO_4$, which is reflected in the large distortion of the WO_4 tetrahedra in this phase. The larger distortion of the WO_4 tetrahedra in fergusonite $PbWO_4$, as compared to the fergusonite phase of alkaline-earth tungstates, is opposite to that in scheelite-

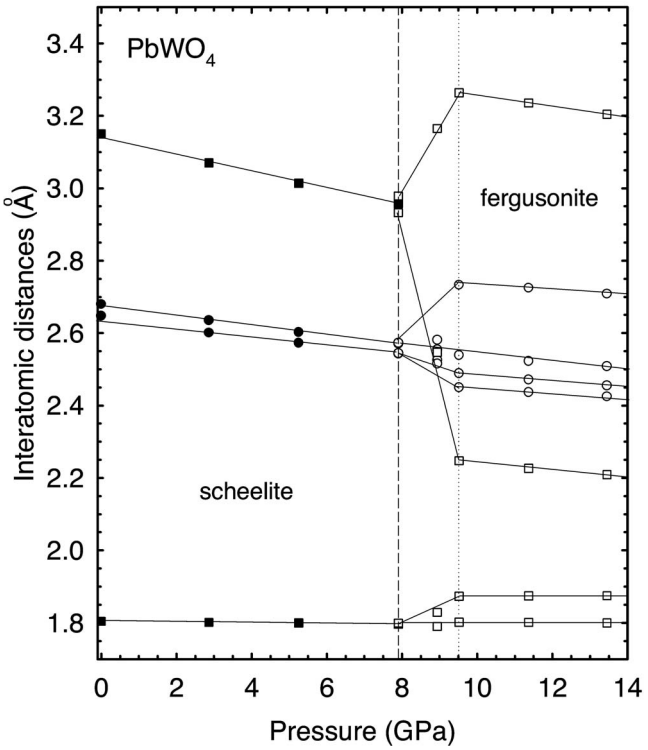

FIG. 8. W-O (squares) and Pb-O (circles) distances in the scheelite (solid) and fergusonite (empty) phases of $PbWO_4$ at different pressures, as obtained from *ab initio* total-energy calculations after Ref. 12. The dashed line shows the theoretically predicted phase-transition pressure between the scheelite and fergusonite phases. The dotted line shows the division of the fergusonite phase with tetrahedral and octahedral coordination for the W ion.

$PbWO_4$, which exhibits the least distorted WO_4 tetrahedra, as already discussed.

It must be noted that the theoretical knowledge of the behavior W-O bond distances with pressure reported in Fig. 8 for fergusonite $PbWO_4$ allows an estimation of the frequencies and pressure coefficients of the internal stretching modes of the tungstate group in fergusonite $PbWO_4$ by using Eqs. (6) and (7). We are not going to do such a task for the sake of simplicity, but we want to stress that the two additional stretching fergusonite modes observed experimentally at 446 and 471 cm^{-1} at 9 GPa, and that *ab initio* calculations located at 458 and 462 cm^{-1} at 9 GPa, have calculated pressure coefficients considerably larger than those of the other fergusonite modes (see Table III). These large pressure coefficients can be understood if we consider that the estimated W-O bond distances associated to these two modes (2.10 and 2.13 Å at 9 GPa) correspond to the W-O bond distance theoretically calculated at 2.25 Å at 9.5 GPa (see Fig. 8). The large pressure coefficients of the above two modes are coherent with the large decrease of the associated W-O bond length under compression due to the distortion of the tungstate group observed in Fig. 8. Note that in $BaWO_4$ the corresponding fergusonite modes (calculated to be at 362 and 363 cm^{-1} at 7.5 GPa) have rather similar calculated pressure coefficients than the other fergusonite modes.[10]

Another conclusion that can be drawn from the fact that the fergusonite phase of $PbWO_4$ is a structure acting as a bridge between 4 and 6 coordination for W, is that maybe modes of the fergusonite phase overlap with modes of the $PbWO_4$-III phase due to the small distortion between both phases. This fact makes even more difficult the assignment of modes of both phases. The above conclusion could be supported by: (1) the small fading rate of some fergusonite modes above 10 GPa; (2) the appearance of a few $PbWO_4$-III modes above 12.6 GPa; and (3) the observation of some fergusonite modes (much weaker in intensity than the mode at 870 cm^{-1} at 9 GPa) up to pressures of 14.6 GPa (see Figs. 5–7).

Finally, the application of Hardcastle and Wachs' rules to the $PbWO_4$-III phase can help in assigning the first-order modes of this low-symmetry phase provided that the WO_6 octahedra can be regarded as almost independent units.[43] In the characterization of the $PbWO_4$-III structure at 1 atm, the following W-O distances were reported:[7] 1.76, 1.79, 1.81, 1.81, 1.83, 1.88, 1.91, 2.03, 2.10, 2.16, 2.17, and 2.26 Å. The average distances of Ref. 7 at 1 atm taken in pairs are 1.775, 1.81, 1.855, 1.97, 2.13, and 2.22 Å, and Eq. (7) allows us to obtain the following Pauling's bond strengths in v.u.: 1.75, 1.5, 1.23, 0.76, 0.41, 0.29. Altogether they sum 5.9 v.u., which fits nicely the formal valence of the W^{6+} ion.[43] Therefore, this result clearly suggests that W has an octahedral coordination in the $PbWO_4$-III phase and that the W-O bond distances reported in Ref. 7 could be used to estimate the stretching modes of the $PbWO_4$-III phase. With the data of Ref. 7 and Eq. (6) we have calculated the stretching frequencies 908, 858, 826, 795, 723, 683, 543, 458, 424, 416, and 351 cm^{-1}. These values agree qualitatively with the average positions of the stretching modes calculated at 9 GPa by first principles and with our assignments of the $PbWO_4$-III Raman peaks (see Tables IV and V and Figs. 6 and 7).

D. Phase transitions in other related compounds

The Raman spectrum of monoclinic $HgWO_4$ at 1 atm (Ref. 45) can also be compared to Raman spectra of $PbWO_4$ above 8 GPa, as already done in Ref. 10 for alkaline-earth tungstates. Since the monoclinic structure of $HgWO_4$ exhibits octahedral W coordination, $HgWO_4$ is expected to share some characteristics of the fergusonite phase in $PbWO_4$, which has 4+2 coordination for W. In this sense, the smallest high-frequency stretching mode near 700 cm^{-1} in $HgWO_4$ is similar to the 693 cm^{-1} mode in fergusonite $PbWO_4$ at 9 GPa. Furthermore, the low-frequency modes near 500 cm^{-1} in $HgWO_4$ likely arise from the scheelite $\nu_4(B_g+E_g)$ modes, and could be stretching modes like those found near 470 cm^{-1} in fergusonite $PbWO_4$. We think that the similar stretching-mode frequencies around 500 and 700 cm^{-1} in fergusonite $PbWO_4$ and $HgWO_4$ are features related to the reduction of the phonon gap of the scheelite and fergusonite phases caused by the tendency of W to octahedral coordination in these two tungstates with high electronegative A cations like Hg and Pb, where *d* orbitals can also play a significant role. In any case, new and more detailed *RT* Raman spectra of monoclinic $HgWO_4$ would be of help in the definite assignment of all its modes, especially in the low-frequency region.

We would like to highlight also that the pressure-driven transitions for scheelite $PbWO_4$ could be the same as those for scheelites $AgReO_4$ and $PbMoO_4$. This conclusion is obtained on the basis of the positions of the three compounds in Bastide's diagram[46] and on the similarities of their high-pressure Raman spectra. In the case of $AgReO_4$, we can compare it directly to $PbWO_4$ since Raman spectra up to 18 GPa were previously reported by J. W. Otto *et al.*[47] However, in the case of $PbMoO_4$ the lack of detailed Raman spectrum at high pressures allows us to discuss it only on the basis of the reported frequencies of the high-pressure phases.[9] Both scheelite $AgReO_4$ and $PbMoO_4$ are located in the south direction with respect to $PbWO_4$ in Bastide's diagram, therefore on the basis of the northeast rule for a pressure increase in Bastide's diagram[46] one can predict a larger stability of the scheelite phase in these compounds than in $PbWO_4$, as indeed observed. The scheelite phase in $PbMoO_4$ is found up to 9.5 GPa, and that of $AgReO_4$ is observed up to 11 GPa. We can interpret the Raman spectra of $PbMoO_4$ and $AgReO_4$ on the basis of: (1) the comparison of the scheelite frequencies and pressure coefficients of both compounds with those of $PbWO_4$, and (2) the comparison of the high-pressure spectrum of $AgReO_4$ at 14 GPa and the spectra of $PbWO_4$ between 9 and 10 GPa.

Regarding the scheelite phase, the spectra of the three compounds exhibit similar bands with similar frequencies and pressure dependences: (1) there is a gap between the external *T* and *R* modes, being this gap is larger in $PbWO_4$ and $PbMoO_4$ than in $AgReO_4$; and (2) the pressure coefficients of the scheelite stretching modes in these compounds do not scale with the length of the *c* axis, as it occurs in the alkaline-earth tungstates and in alkaline perrhenates.[47] The above similarities between the modes of these compounds are likely due to similar electronegativities of the Ag and Pb cations, that lead to negligible charge-transfer effects be-

tween the A^{2+} cation and the BO_4^{2-} anion and consequently to low frequencies and pressure coefficients of the internal BO_4 modes due to the weakness of the W-O bond as already discussed in $PbWO_4$.

The main differences between the scheelite phases of the three compounds are: (1) the frequencies of the internal stretching modes of ReO_4 tetrahedra are higher than those of the WO_4 and MoO_4 tetrahedra, as already noted in the discussion of the ionicity of $PbWO_4$. This is due to the larger stretching force constant of ReO_4 tetrahedra as a consequence of the shorter Re-O bond distances compared to the W-O and Mo-O bond distances; (2) the pressure coefficients of all external modes are somewhat larger in $AgReO_4$. In fact the lowest $T(B_g)$ mode does not exhibit a negative-pressure coefficient in $AgReO_4$ as in the studied tungstates and molybdates. This is in agreement with the larger stability of the scheelite structure in the perrhenate; and (3) the scheelite $\nu_1(A_g)$ mode shows a very small pressure coefficient in $PbMoO_4$ and $AgReO_4$, thus suggesting a negligible decrease of the B-O bond distance in these compounds.

We believe that these similarities and differences in the scheelite phases of the three compounds can also be traced in the high-pressure Raman spectra of $PbWO_4$ and $AgReO_4$. Phase transitions between 11 and 14 GPa are reported in $AgReO_4$ which exhibits a high-frequency mode at 942 cm^{-1} whose intensity decreases strongly above 14 GPa, like the 870 cm^{-1} mode in fergusonite $PbWO_4$. Furthermore, two modes located at 275 and 301 cm^{-1} at 14 GPa in $AgReO_4$ exhibit a nearly zero-pressure coefficient like the $PbWO_4$ -III modes located at 288 and 305 cm^{-1} at 13.7 GPa. Finally, we must note that there is a broadband composed of three peaks near 220 cm^{-1} in $AgReO_4$ that resembles that of the $PbWO_4$-III phase near 200 cm^{-1}. A closer comparison cannot be made due to the lack of more detailed spectra of $AgReO_4$, especially in the 450 to 850 cm^{-1} region.

The main differences between the high-pressure phases of the three compounds are the following ones. Assuming that in $PbMoO_4$ there is a phase transition to the fergusonite phase around 9.5 GPa, and that in $AgReO_4$ there is a first phase transition to the fergusonite phase around 11 GPa and a second phase transition to the $PbWO_4$-III phase around 14 GPa, a striking difference between the high-pressure Raman spectrum of the three compounds is that the change in frequency of the fergusonite high-frequency stretching A_g mode with respect to the scheelite $\nu_1(A_g)$ mode is very small in $PbMoO_4$ and in $AgReO_4$ (at most 4 cm^{-1}), unlike in $PbWO_4$. Therefore, the fergusonite phases of $PbMoO_4$ and $AgReO_4$ resemble more those of alkaline-earth tungstates and likely retain the tetrahedral coordination from Mo and Re cations.[10] This result suggests that the jump between these two modes at the scheelite-to-fergusonite phase transition in $PbWO_4$ due to the internal distortions revealed by *ab initio* calculations is particular for $PbWO_4$ and is not usually found in other scheelites. On the other hand, two new and strong peaks are observed above 14 GPa in the Raman spectrum of $AgReO_4$. One is at 71 cm^{-1} and the other is around 951–953 cm^{-1}. These two modes maintain their intensities at the highest pressures, while the 942 cm^{-1} mode assigned to the fergusonite phase fades. We think that these two peaks could correspond to the $PbWO_4$-III phase of $AgReO_4$. However, only one strong high-frequency peak is observed in this phase, unlike the two strong high-frequency peaks observed in $PbWO_4$. This fact can be due to the limited resolution of the Raman spectra of $AgReO_4$, but it also could be due to a transition to another monoclinic structure with less formula units per unit cell, like the $LaTaO_4$ structure. The hypothesis stated above is valid for $PbMoO_4$, which exhibits three modes near the scheelite $\nu_1(A_g)$ mode and two more modes near the scheelite ν_3 modes after the phase transition at 9.5 GPa. The three modes near the scheelite $\nu_1(A_g)$ mode are compatible with the assignment of one of them to the fergusonite phase, and the remaining two modes to the $PbWO_4$-III phase. In any case, further Raman studies in $PbMoO_4$ and $AgReO_4$ are needed to fully understand the pressure behavior of these two scheelites.

V. CONCLUSIONS

We performed *RT* Raman-scattering measurements under pressure in $PbWO_4$ up to 17 GPa. The frequency pressure dependence of all the first-order modes of the scheelite phase (stolzite) have been measured. We have observed the onset of the scheelite-to-$PbWO_4$-III phase transition around 6.2 GPa in good agreement with the theoretically calculated value of the I/III coexistence pressure (5.3 GPa).[12] Our measurements show that the transition to the $PbWO_4$-III phase is not completed up to 14.6 GPa. We have also found a scheelite-to-fergusonite phase transition at 7.9 GPa in complete agreement with earlier experimental and theoretical studies.[12] In summary, we have observed the following structural sequences in $PbWO_4$: (1) scheelite from 1 atm to 6.2 GPa; (2) scheelite+$PbWO_4$-III (partial transition) between 6.2 and 7.9 GPa; (3) scheelite+$PbWO_4$-III+fergusonite between 7.9 and 9.0 GPa; (4) $PbWO_4$-III+fergusonite from 9.5 GPa to 14.6 GPa; (5) $PbWO_4$-III above 15 GPa. On decreasing pressure from 17 GPa the scheelite structure of $PbWO_4$ is recovered below 5 GPa in agreement with ADXRD measurements.[12]

The observation of the scheelite-to-fergusonite transition at pressures above that for the scheelite-to-$PbWO_4$-III transition can only be explained by the kinetic hindrance of the reconstructive scheelite-to-$PbWO_4$ phase transition due to its slow kinetics likely caused by an activation barrier, and the displacive second-order nature of the scheelite-to-fergusonite phase transition, as already pointed out in Refs. 10, 12, and 42. As a consequence of this, we have found the coexistence of the scheelite, fergusonite, and $PbWO_4$-III phases in the pressure range of 7.9 to 9 GPa and the coexistence of the last two phases up to 14.6 GPa, despite most of the fergusonite modes disappear above 12.6 GPa. These results allow us to understand previous x-ray diffraction results.[12] The Raman peaks of the $PbWO_4$-III phase appear before those of the fergusonite, but once the fergusonite phase appears, its Raman peaks are stronger than those of $PbWO_4$-III and dominate the spectrum up to 12.6 GPa, pressure at which the $PbWO_4$-III phase dominates over the fergusonite. This result explains why in the ADXRD study[12] the fergusonite phase was observed at 9 GPa and why the ADXRD pattern of the $PbWO_4$-III phase appears only after the fergusonite phase extinguishes above 14.6 GPa.

Additionally, we have performed *ab initio* lattice-dynamics calculations of $PbWO_4$ at selected pressures in the scheelite, fergusonite, and $PbWO_4$-III phases. Our calculated frequencies in the three structures agree with the frequencies of the observed Raman modes and have allowed the assignment and discussion of the nature of many modes in the three phases. We have found that scheelite $PbWO_4$ (stoltzite) is the less ionic tungstate and this yields important consequences for the estimation of the vibrations of the quasifree WO_4 molecule. We have found that $PbWO_4$ under pressure behaves in a similar way than $BaWO_4$.[10] With the aid of Hardcastle and Wachs', and of Brown and Wu's formulas and *ab initio* calculations, we have shown that the WO_4 tetrahedra in scheelite $PbWO_4$ become distorted in fergusonite $PbWO_4$. The distortion leads to a change of interatomic W-O distances in fergusonite $PbWO_4$, which suggests that this phase acts as a bridge between fourfold and sixfold W coordination. The distortion of the W-O bonds of the fergusonite phase in $PbWO_4$, evidenced by *ab initio* calculations, explains the big decrease of the frequency of one of the Raman-stretching modes of this phase, and why the scheelite-to-fergusonite transition is observed in XANES measurements while the fergusonite-to $PbWO_4$-III transition is faintly observed in XANES measurements.[12] Furthermore, we have shown that the $PbWO_4$-III phase has octahedral coordination for the W cation, and that the WO_6 octahedra in the fergusonite and $PbWO_4$-III phases can be regarded as almost independent units.

Finally, the comparison of the pressure behavior of $PbWO_4$ with $PbMoO_4$, and with $AgReO_4$ and the possible similar phase transitions in the three compounds according to Bastide's diagram suggests that data of $AgReO_4$ under pressure should be revised and new measurements on $PbMoO_4$ under pressure need to be made in order to check if these three compounds suffer similar phase transitions.

ACKNOWLEDGMENTS

The authors thank P. Lecoq (CERN) for providing the $PbWO_4$ crystals used in this study and A. Cantarero (Institute of Materials Science, University of Valencia) for providing access to the experimental Raman setup. This work was made possible through financial support of the MCYT of Spain under Grants No. MAT2004-05867-C03-01/03 and No. MAT2002-04539-C02-02. F.J.M. acknowledges financial support by the "*Programa Incentivo a la Investigacion de la U.P.V.*" D.E. and N.G. acknowledge financial support from the MCYT of Spain through the "Ramon y Cajal" program. The use of the computational resources of the Barcelona Supercomputing Center (Mare Nostrum) for the DFT calculations is also gratefully acknowledged. J.L.S., A.M., and P.R-H. acknowledge financial support from the Consejería de Educación del Gobierno Autónomo de Canarias (Grant No. PI2003/074).

*Corresponding author. Present address at UPV. Fax: +34 96 387 71 89. Electronic address: fjmanjon@fis.upv.es

[1] A. A. Kaminskii *et al.*, Opt. Commun. **183**, 277 (2000).
[2] M. Kobayashi, M. Ishii, Y. Husuki, and H. Yahagi, Nucl. Instrum. Methods Phys. Res. A **333**, 429 (1993).
[3] P. Lecoq, I. Dafinei, E. Auffray, M. Schneegans, M. V. Korzhik, O. V. Missevitch, V. B. Pavlenko, A. A. Fedorov, A. N. Annenkov, V. L. Kostylev, and V. D. Ligun, Nucl. Instrum. Methods Phys. Res. A **365**, 291 (1995).
[4] A. W. Sleight, Acta Crystallogr., Sect. B: Struct. Crystallogr. Cryst. Chem. **28**, 2899 (1972).
[5] T. Fujita, I. Kawada, and K. Kato, Acta Crystallogr., Sect. B: Struct. Crystallogr. Cryst. Chem. **33**, 162 (1977).
[6] M. Itoh and M. Fujita, Phys. Rev. B **62**, 12825 (2000).
[7] P. W. Richter, G. J. Kruger, and C. W. F. T. Pistorius, Acta Crystallogr., Sect. B: Struct. Crystallogr. Cryst. Chem. **32**, 928 (1976).
[8] A. Jayaraman, B. Batlogg, and L. G. Van Uitert, Phys. Rev. B **28**, 4774 (1983).
[9] A. Jayaraman, B. Batlogg, and L. G. Van Uitert, Phys. Rev. B **31**, 5423 (1985).
[10] F. J. Manjón, D. Errandonea, N. Garro, J. Pellicer-Porres, P. Rodríguez-Hernández, S. Radescu, J. López-Solano, A. Mujica, and A. Muñoz, Phys. Rev. B **74**, 144111 (2006).
[11] D. Errandonea, J. Pellicer-Porres, F. J. Manjón, A. Segura, Ch. Ferrer-Roca, R. S. Kumar, O. Tschauner, P. Rodríguez-Hernández, J. López-Solano, S. Radescu, A. Mujica, A. Muñoz, and G. Aquilanti, Phys. Rev. B **72**, 174106 (2005).
[12] D. Errandonea, J. Pellicer-Porres, F. J. Manjón, A. Segura, Ch. Ferrer-Roca, R. S. Kumar, O. Tschauner, J. López-Solano, P. Rodríguez-Hernández, S. Radescu, A. Mujica, A. Muñoz, and G. Aquilanti, Phys. Rev. B **73**, 224103 (2006).
[13] D. Errandonea, F. J. Manjón, M. Somayazulu, and D. Häusermann, J. Solid State Chem. **177**, 1087 (2004).
[14] D. Errandonea, D. Martinez-Garcia, R. Lacomba-Perales, J. Ruiz-Fuertes, and A. Segura, Appl. Phys. Lett. **89**, 091901 (2006).
[15] A. Grzechnik, W. A. Chrichton, W. G. Marshall, and K. Friese, J. Phys.: Condens. Matter **18**, 3017 (2006).
[16] A. A. Annenkov, M. V. Korzhik, and P. Lecoq, Nucl. Instrum. Methods Phys. Res. A **490**, 30 (2002).
[17] J. M. Moreau, P. Galez, J. P. Peigneux, and M. V. Korzhik, J. Alloys Compd. **238**, 46 (1996).
[18] Y. Shen, R. S. Kumar, M. Pravica, and M. F. Nicol, Rev. Sci. Instrum. **75**, 4450 (2004).
[19] G. Kresse *et al.*, computer code VASP. For more information see http://cms.mpi.univie.ac.at/vasp
[20] G. Kresse and D. Joubert, Phys. Rev. B **59**, 1758 (1999).
[21] D. L. Rousseau, R. P. Baumann, and S. P. S. Porto, J. Raman Spectrosc. **10**, 253 (1981).
[22] S. P. S. Porto and J. F. Scott, Phys. Rev. **157**, 716 (1967).
[23] G. Herzberg, *Molecular Spectra and Molecular Structure: II Infra-Red and Raman Spectra* (D. Van Nostrand Co. Inc., New York, 1945).
[24] J. M. Stencel, J. Springer, and E. Silberman, J. Mol. Struct. **41**, 11 (1977).
[25] S. Bastians, G. Crump, W. P. Griffith, and R. Withnall, J. Raman

Spectrosc. **35**, 726 (2004).
[26] D. Christofilos, K. Papagelis, S. Ves, G. A. Kourouklis, and C. Raptis, J. Phys.: Condens. Matter **14**, 12641 (2002).
[27] D. Christofilos, S. Ves, and G. A. Kourouklis, Phys. Status Solidi B **198**, 539 (1996).
[28] M. Liegegois-Duyckaerts and P. Tarte, Spectrochim. Acta, Part A **28**, 2037 (1972).
[29] N. Weinstock, H. Schulze, and A. Müller, J. Chem. Phys. **59**, 5063 (1973).
[30] A. N. Akimov, M. V. Nikanovich, V. G. Popov, and D. S. Umreiko, J. Appl. Spectrosc. **45**, 806 (1987).
[31] F. M Pontes, M. A. M. A. Maurera, A. G. Souza, E. Longo, E. R. Leite, R. Magnani, M. A. C. Machado, P. S. Pizani, and J. A. Varela, J. Eur. Ceram. Soc. **23**, 3001 (2003).
[32] M. Nicol and J. F. Durana, J. Chem. Phys. **54**, 1436 (1971).
[33] N. Ganguly and M. Nicol, Phys. Status Solidi B **79**, 617 (1977).
[34] K. J. Dean and G. R. Wilkinson, J. Mol. Struct. **79**, 293 (1982).
[35] K. Nakamoto, *Infrared and Raman Spectra of Inorganic and Coordination Compounds*, 3rd ed. (Wiley, New York, 1978).
[36] F. Gonzalez-Vilchez and G. W. Griffith, J. Chem. Soc. Dalton Trans., **1976**, 1416 (1972).
[37] R. Moret, P. Launois, T. Wagberg, and B. Sundqvist, Eur. Phys. J. B **15**, 253 (2000).
[38] M. Gnyba, M. Keränen, M. Kozanecki, R. Bogdanowicz, B. B. Kosmowski, and P. Wroczynski, Opto-Electron. Rev. **10**, 137 (2002).
[39] D. M. Datelbaum, J. D. Jensen, A. M. Schwendt, E. M. Kober, M. W. Lewis, and R. Menikoff, J. Chem. Phys. **122**, 144903 (2005).
[40] V. Panchal, N. Garg, and S. M. Sharma, J. Phys.: Condens. Matter **18**, 3917 (2006).
[41] D. Christofilos, J. Arvanitidis, E. Kampasakali, K. Papagelis, S. Ves, and G. A. Kourouklis, Phys. Status Solidi B **241**, 3155 (2004).
[42] D. Errandonea, Physica B (to be published).
[43] F. D. Hardcastle and I. E. Wachs, J. Raman Spectrosc. **26**, 397 (1995).
[44] I. D. Brown and K. K. Wu, Acta Crystallogr., Sect. B: Struct. Crystallogr. Cryst. Chem. **32**, 1957 (1976).
[45] G. Blasse, J. Inorg. Nucl. Chem. **37**, 97 (1975).
[46] J. P. Bastide, J. Solid State Chem. **71**, 115 (1987).
[47] J. W. Otto, J. K. Vassiliou, R. F. Porter, and A. L. Ruoff, Phys. Rev. B **44**, 9223 (1991).